To the Graduate Council:

I am submitting herewith a thesis written by Edward Thomas Tomlinson entitled "Approximate Numerical Solutions to the Time-Dependent Neutron Transport Equation using the TASK Algorithm." I recommend that it be accepted in partial fulfillment of the requirements for the degree of Master of Science, with a major in Nuclear Engineering.

J. C. Robinson

J. C. Robinson, Major Professor

We have read this thesis and recommend its acceptance:

Paul N Stevens

P.F. Pasqua

F.W. Kerlin

D. D. Flanagan

Accepted for the Council:

Hilton A. Smith

Vice Chancellor
Graduate Studies and Research

APPROXIMATE NUMERICAL SOLUTIONS TO THE TIME-DEPENDENT NEUTRON TRANSPORT EQUATION USING THE TASK ALGORITHM

A Thesis

Presented for the

Master of Science

Degree

The University of Tennessee

Edward Thomas Tomlinson

June 1974

ACKNOWLEDGMENTS

The work was performed in the Neutron Physics Division of the Oak Ridge National Laboratory which is operated by Union Carbide Corporation for the United States Atomic Energy Commission. Financial support for this work was provided in the form of a research assistantship from The University of Tennessee through Oak Ridge National Laboratory.

The author wishes to express his appreciation to the individuals who contributed to various phases of this work.

Dr. J. C. Robinson, who served as advisor, suggested the topic and provided invaluable guidance throughout the work.

W. W. Engle and W. A. Rhoades of Oak Ridge National Laboratory, provided encouragement through many stimulating discussions with the author. W. W. Engle also provided cross section data and the Time-Dependent ANISN test problem.

R. A. Lillie and D. B. Simpson provided valuable background information and assistance in creating a working computer code.

Finally, the author would like to thank his wife, Rosemary, for her patience during the course of this work. This thesis is dedicated entirely to her.

1147251

ABSTRACT

The purpose of this work is to develop a method for obtaining approximate solutions to the time-dependent Boltzmann neutron transport equation. A transfer-scattering algorithm is used to solve the equation in the spatial, energy, and angular domains. The temporal operator is removed by assuming the neutron flux behaves as the product of a linear function and an exponential function between two given time planes. This assumed behavior is substituted into the multigroup, one-dimensional, slab geometry discrete ordinate form of the transport equation. The resultant equations are forward differenced and then cast into a form making them amenable to solution by the transfer-scattering algorithm.

An exponential extrapolation of the flux is used as a convergence acceleration device. An approximation is made for the magnitude of rod drop transients to alleviate the need to use small time steps during the initial transient.

Finally, a number of numerical experiments are performed to illustrate the validity of the method. These results are compared with results obtained from already existing methods. In all cases, agreement is excellent.

TABLE OF CONTENTS

CHAPTER		PAGE
I.	INTRODUCTION	1
	Reactor Kinetics Calculations	1
	A Review of Pertinent Numerical Techniques	2
	Time-Dependent ANISN (TDA)	2
	TIMEX	5
	Scope and Organization	8
II.	REVIEW OF THE TRANSFER-SCATTERING ALGORITHM	9
	Transfer-Scattering Algorithm	9
	Outer Iteration Techniques	17
III.	TIME-DEPENDENT TASK SOLUTION SCHEME	20
	Development of the Numerical Model	20
	The Point Kinetics Approximation	29
	Numerical Procedures	31
IV.	NUMERICAL RESULTS	34
	Comparison with Point Kinetics	34
	Comparison with TDA	42
V.	SUMMARY	47
	Conclusions	47
	Recommendations	47
BIBLIOGRAPHY		49
APPENDIX		52
VITA		64

LIST OF TABLES

TABLE PAGE

I. Interpretation of the Spatially Dependent Test Case 41

LIST OF FIGURES

FIGURE		PAGE
1.	Calculational Model--Half Core Model of FTR-3m	35
2.	Relative Reactor Power Versus Time--TDT and Point Kinetics Calculations--Far Subcritical	37
3.	Relative Reactor Power Versus Time--TDT and Point Kinetics Calculations--Near Critical	38
4.	Relative Reaction Rates Versus Time--TDT and Point Kinetics Calculations	40
5.	Calculational Model--Half Core Model for TDA Test Problem .	44
6.	Relative Reactor Power Versus Time--TDT and TDA Calculations	45

CHAPTER I

INTRODUCTION

I. REACTOR KINETICS CALCULATIONS

The early kinetics models used simplified "point kinetics" equations to describe the kinetic behavior of nuclear systems. The applicability of this model is considered to be limited to systems in which the space and time dependence of the neutron flux can be separated[1]. Reactors with small closely coupled cores may be able to be approximated with the point kinetic model.

Reactors with large loosely coupled cores must be analyzed with more detailed treatments of the space and time dependent neutron flux. A localized perturbation may cause a large variation on the flux near the site of the perturbation and only a small variation elsewhere. The effect of this perturbation averaged over the entire reactor may be small; however, the failure to consider these localized effects may result in design specifications being exceeded in the neighborhood of the perturbations.

Improvement of calculational methods and models led to space and energy-dependent models. Most of these models employed some variation of multigroup diffusion theory. Although the diffusion model was an improvement over point kinetics, these models were still limited by the diffusion approximation.

Current designs for the liquid metal cooled fast breeder reactor employ ex-vessel detectors to monitor the subcriticality of the system. Experience has shown that transport theory yields acceptable results for this type of deep penetration problem. Results of calculations performed using diffusion theory are unacceptable[2].

A major factor limiting the use of transport theory, until recently, is that it requires relatively large amounts of computational time and computer storage. The advent of relatively large fast computers has made practical the use of transport codes for reactor kinetics calculation.

II. A REVIEW OF PERTINENT NUMERICAL TECHNIQUES

The purpose of this section is to present a brief review of some of the existing techniques used in solving the multigroup time-dependent transport equation. Some of the inherent difficulties of each method will also be discussed.

Time-Dependent ANISN (TDA)

The one dimensional time-dependent, finite difference form of the Boltzmann transport equation programmed in TDA* is given by[3]

$$\frac{V}{v\Delta t}\left(N_{t+1} - N_t\right) + \mu\left(A_{i+1}N_{i+1} - A_iN_i\right)$$

$$+ \frac{1}{w}\left(\alpha_{m+1}N_{m+1} - \alpha_mN_m\right) + \Sigma vN = SV \qquad (1\text{-}1)$$

---

*The following acronyms are used throughout this work to denote computer codes:

TASK - Transfer and Scattering Kinetics
TDA - Time - Dependent ANISN
TDT - Time - Dependent TASK

where

V = volume of space interval i,

v = particle velocity,

Δt = width of the time interval,

μ = direction cosine,

w = weight associated with direction μ,

A_i = area of interface between space intervals,

α_m = curvature term to account for changes of direction during particle streaming across a curved space interval,

Σ = total cross section,

S = source (including fixed, fission, and scattered sources), and

N = particle fluxes to be determined.

The convention of omitting the subscripts on the cell centered terms has been followed. The subscripts i, m, g and t refer to space interval, angle increment, energy group, and time interval, respectively.

Seven fluxes appear in Equation (1-1). Three of them are known from boundary conditions or from previous calculations in adjoining mesh intervals. To determine the remaining fluxes, three additional equations relating the three known and the four unknown fluxes must be derived. For stability and generality, the weighted difference equations are used in TDA[4]:

$$N = aN_{t+1} + (1-a)\,N_t = bN_{i+1} + (1-b)N_i$$

$$= cN_{m+1} + (1-c)N_m \,. \qquad (1\text{-}2)$$

If the constant a, b, and c are each equal to 0.5, the weighted difference equations are equivalent to the ordinary diamond difference equations. If a, b, and c are equal to 1.0, the weighted difference equations reduce to the step difference equations.

The unknown fluxes can be solved by substituting Equations (1-2) into Equation (1-1). To insure that the fluxes are positive and the values of a, b, and c are approximately 0.5, the following equations are used to solve for a, b, and c:

$$1 - a = (V/v\Delta t + SV/N_t)/[\Sigma V + |\mu|(A_{i+1} + A_i)] \ , \qquad (1\text{-}3a)$$

$$1 - b = (|\mu|A_{i+1} + SV/N_{i+1})/[\Sigma V + |\mu|(A_{i+1} - A_i) + 2V/v\Delta t] \ , \qquad (1\text{-}3b)$$

and

$$1 - c = (\alpha_m/w + SV/N_m)/(\Sigma v + 2V/v\Delta t) \ . \qquad (1\text{-}3c)$$

The use of large time steps for which

$$\frac{1}{\Sigma_a v} << \Delta t$$

when used in connection with the weighted difference equations have been found to cause the iteration scheme to converge to erroneous results[5]. The truncation error of the diamond difference scheme exhibits a divergent characteristic under certain conditions of space and time mesh sizes related by the ratio

$$p = \frac{v\Delta t}{\Delta r} \ , \qquad (1\text{-}4)$$

where Δr represents the width of the spatial interval. For $p > 1$, the diamond difference equations produce poor results. The weighted difference equations which are encoded in TDA are relatively insensitive to the ratio p. This is attributed to their arbitrary positioning of the cell averaged flux.

TIMEX[6]

The multigroup neutron transport equation can be written in the matrix form

$$V^{-1} \frac{\partial}{\partial t} \psi = -B\psi + q \ . \tag{1-5}$$

The vector ψ contains the unknown angular fluxes in each energy group as a function of time t, position r, and direction Ω. The diagonal matrix V contains the neutron velocities and the vector q contains inhomogeneous sources. The defining equations for the linear operator B are:

$$B\psi = (L-S)\psi \ , \tag{1-6a}$$

$$(L\psi)_g = \Omega \cdot \nabla\psi_g + \sigma(r)\psi_g \ , \tag{1-6b}$$

and

$$(S\psi)_g = \sum_{g'} \int d\Omega' \kappa(r;g',\Omega' \rightarrow g,\Omega)\psi_{g'}(r,\Omega') \ . \tag{1-6c}$$

The subscript g denotes the gth component of subscripted vectors.

The following equation is the difference approximation to the gth member of Equation (1-5):

$$\frac{1}{v}\left(\frac{\psi^{j+1} - \psi^{j}}{\Delta t}\right) + \mu_m \left(\frac{A_{i+1/2}\psi^{j+1}_{i+1/2} - A_{i-1/2}\psi^{j+1}_{i-1/2}}{V_i}\right)$$

$$+ \left(\frac{\alpha_{m+1/2}\psi^{j+1}_{m+1/2} - \alpha_{m-1/2}\psi^{j+1}_{m-1/2}}{w_m V_i}\right) + \sigma_i \psi^{j+1}$$

$$= S^{j}_{m,i} + q_{m,i} \qquad (1\text{-}7)$$

where the group subscripts have been omitted. The notation used is:

v = group velocity,

Δt = time step size,

$A_{i+1/2}$ = area of cell face,

V_i = cell volume,

w_m = quadrature weights,

$\alpha_{m+1/2}$ = curvature coefficients,

σ_i = total cross section

$S^{j}_{m,i}$ = scattering and fission sources computed from the jth time level, and

$q_{m,i}$ = inhomogeneous sources.

To solve Equation (1-7) for ψ^{j+1} given ψ^{j}, it is necessary to make an assumption concerning the shape of the flux over a mesh cell. The following relations are used:

$$\psi^{j+1} = \frac{\psi^{j+1}_{i+1/2} + \psi^{j+1}_{i-1/2}}{2} \qquad (1\text{-}8a)$$

$$\psi^{j+1} = \frac{\psi^{j+1}_{m+1/2} + \psi^{j+1}_{m-1/2}}{2} . \qquad (1\text{-}8b)$$

The j+1 time step flux can be solved for explicitly using Equations (1-7), (1-8a), and (1-8b).

There are two acceleration techniques available in TIMEX, rebalance and extrapolation. Both methods are usually stable, but there are circumstances under which the rebalance method can lead to an unstable algorithm. Only the extrapolation method will be considered in this thesis.

The extrapolation method[7] assumes that the flux can be written as

$$\psi(t) = e^{\omega t}\phi(t) \ , \qquad (1\text{-}9)$$

where ω is a diagonal matrix and the function ϕ is a small modulation of the assumed exponential behavior. (Details of this type method appear in the next chapter.)

The extrapolation method is a special kind of predictor-corrector method. It is especially appropriate in situations where the time variation of the flux is smooth and nearly exponential. These conditions are usually true at long times following some initial transient providing the cross sections and source remain constant with time.

Each technique has its own calculational difficulties. In the TDA technique, there is the necessity to do both inner and outer iterations. There is also an interdependence of the spatial mesh and the time mesh. The TIMEX technique is susceptible to errors introduced by its non-iterative characteristic.

III. SCOPE AND ORGANIZATION

The objective of this thesis is to develop a numerical technique which will incorporate the best features of the two previously discussed techniques and to introduce some approximations to alleviate some of the calculational difficulties. In particular, the method will be iterative, but will not require inner iterations. The interative technique will incorporate a flexible energy group structure and an exponential extrapolation of the time-dependent flux. Point kinetics will be used to approximate the magnitude of the flux change during a rod drop, eliminating the need to use small time steps during the initial transient. General transient analysis can be carried out using the standard difference techniques.

In Chapter II, a brief review of the transfer-scattering algorithm developed by Dodds[8,9] and the associated outer iteration scheme developed by Lillie[10] are presented. Chapter III presents the development of the time dependent difference equations. In Chapter IV, results of calculations performed for a modified mock-up of Fast Test Reactor-3 (FTR-3m)* are compared with the point kinetics model. Results are also compared to a simple TDA calculation. Chapter V presents the conclusions and a number of recommendations for future work.

---

*FTR-3m denotes an extended shield mock-up of the FTR-3 loading of the ZPR-9 at Argonne National Laboratory.

CHAPTER II

REVIEW OF THE TRANSFER-SCATTERING ALGORITHM

This chapter will present a brief review of the transfer-scattering algorithm and its associated outer iteration scheme. The algorithm was originally developed to obtain approximate solutions to the Laplace transformed neutron transport equation. The development presented in this thesis will parallel the original development with emphasis on its applicability to the time dependent problem.

I. TRANSFER-SCATTERING ALGORITHM

The multigroup discrete ordinate transport equation can be written as,

$$\frac{\partial}{\partial x}\phi_{gd}(x) + \frac{1}{\mu_d}\left[\sum_{g'=1}^{G}\sum_{d'=1}^{D}\Sigma_{g'}\delta_{gg'}\delta_{dd'} - \chi_g(\nu\Sigma_f)_{g'}w_{d'} - T_{gd;g'd'}w_{d'}\right]\phi_{gd}(x) = S_{gd}(x)/\mu_d \qquad (2\text{-}1)$$

$g = 1, \ldots, G$; $d = 1, \ldots, D$, for steady state problems. The subscripts g and d denote the energy group and angular segment, respectively. The terms $\delta_{gg'}$ and $\delta_{dd'}$ are Kronecker delta functions.

The introduction of a state vector,* $\underline{\psi}(x)$, and a source vector, $\underline{Z}(x)$, given by

---

*A singly underlined symbol denotes a vector and a doubly underlined symbol denotes a square matrix.

$$\underline{\psi}(x) = [\phi_{11}, \cdots, \phi_{G1}, \cdots, \phi_{gd}, \cdots, \phi_{GD}]^T \tag{2-2a}$$

$$\underline{Z}(x) = [S_{11}/\mu_1, \cdots, S_{G1}/\mu_d, \cdots, S_{gd}/\mu_d, \cdots, S_{GD}/\mu_D]^T \tag{2-2b}$$

allows Equation (2-1) to be written as

$$\frac{\partial}{\partial x} \underline{\psi}(x) + \underline{\underline{B}}\, \underline{\psi}(x) = \underline{Z}(x) \tag{2-3}$$

where the ij'th element of the complex coupling matrix, $\underline{\underline{B}}$, can be written

$$(B)_{ij} = \frac{1}{\mu_d} \{[\Sigma_{g'} \delta_{gg'} \delta_{dd'} - \chi_g (\nu\Sigma_f)_{g'} + T_{gd;\, g'd'} w_{d'}] w_d\} \tag{2-4}$$

by letting $i = G(d-1)+g$ for $g = 1, \cdots, G$; $d = 1, \cdots, D$ and $j = G(d'-1)+g'$ for $g' = 1, \cdots, G$; $d' = 1, \cdots, D$.

To effect an efficient solution algorithm for Equation (2-3), the state vector $\underline{\psi}(x)$ is expanded in a Taylor series about x. By assuming $\underline{\underline{B}}$ and $\underline{Z}(x)$ remain constant over Δx, the coefficients in Equation (2-3) thus resulting in the following matrix equation:

$$\underline{\psi}(x+\Delta x) = \underline{\underline{\Lambda}}^{(1)}(\Delta x)\, \underline{\psi}(x) + \underline{\underline{\Lambda}}^{(2)}(\Delta x)\, \underline{Z}(x) \tag{2-5}$$

where the $\underline{\underline{\Lambda}}^{(1)}$ and $\underline{\underline{\Lambda}}^{(2)}$ matrices are given by

$$\underline{\underline{\Lambda}}^{(1)}(\Delta x) = \sum_{n=0}^{\infty} (-1)^n \frac{[\underline{\underline{B}}\Delta x]^n}{n!}, \tag{2-6a}$$

$$\underline{\underline{\Lambda}}^{(2)}(\Delta x) = \Delta x \sum_{n=0}^{\infty} (-1)^n \frac{[\underline{\underline{B}}\Delta x]^n}{(n+1)!}. \tag{2-6b}$$

Since $\underline{\underline{\Lambda}}^{(1)}(\Delta x)$ relates the $\underline{\psi}$ vector at space point $x + \Delta x$ to the $\underline{\psi}$ vector at x, Equation (2-5) is referred to as the transfer-matrix formulation. In principal Equation (2-5) along with the appropriate boundary conditions can be applied to obtain a solution to Equation (2-3).

However, this procedure will usually fail for two point boundary value problems due to two numerical difficulties. The first of these difficulties arises in the evaluation of $\underline{\underline{\Lambda}}^{(1)}(\Delta x)$ and $\underline{\underline{\Lambda}}^{(2)}(\Delta x)$ using the series representation, Equations (2-6). Dodds[8] eliminated this difficulty by systematically varying Δx to control the magnitude of the largest element in the series. The manner in which this is done is presented in detail in reference (8). The second difficulty occurs when it becomes necessary to generate $\underline{\underline{\Lambda}}^{(1)}$ and $\underline{\underline{\Lambda}}^{(2)}$ for an entire region. This difficulty is circumvented by transforming to a scattering altorithm.

The transformation to a scattering matrix formulation is accomplished by partitioning Equation (2-5) as follows:

$$\begin{pmatrix} \underline{\psi}U(x+\Delta x) \\ \underline{\psi}L(x+\Delta x) \end{pmatrix} = \begin{pmatrix} \underline{\underline{\Lambda}}_{11}^{(1)}(\Delta x) & \underline{\underline{\Lambda}}_{12}^{(1)}(\Delta x) \\ \underline{\underline{\Lambda}}_{21}^{(1)}(\Delta x) & \underline{\underline{\Lambda}}_{22}^{(1)}(\Delta x) \end{pmatrix} \begin{pmatrix} \underline{\psi}U(x) \\ \underline{\psi}L(x) \end{pmatrix} + \begin{pmatrix} \underline{F}U(x) \\ \underline{F}L(x) \end{pmatrix} \tag{2-7}$$

where

$$\begin{bmatrix} \underline{FU}(\Delta x) \\ \underline{FL}(\Delta x) \end{bmatrix} = \begin{bmatrix} \underline{\underline{\Lambda}}_{11}^{(2)}(\Delta x) & \underline{\underline{\Lambda}}_{12}^{(2)}(\Delta x) \\ \underline{\underline{\Lambda}}_{21}^{(2)}(\Delta x) & \underline{\underline{\Lambda}}_{22}^{(2)}(\Delta x) \end{bmatrix} \begin{bmatrix} \underline{ZU}(x) \\ \underline{ZL}(x) \end{bmatrix} . \tag{2-8}$$

In Equation (2-8) U and L refer, respectively, to the upper and lower halves of the considered vector.

Equation (2-7) can be rearranged for two point boundary value problems such that when applied to an entire problem the unknowns appear on the left side and the known boundary conditions appear on the right side:

$$\begin{bmatrix} \underline{\psi}U(x+\Delta x) \\ \underline{\psi}L(x) \end{bmatrix} = \begin{bmatrix} \underline{\underline{G}}_{11}(\Delta x) & \underline{\underline{G}}_{12}(\Delta x) \\ \underline{\underline{G}}_{21}(\Delta x) & \underline{\underline{G}}_{22}(\Delta x) \end{bmatrix} \begin{bmatrix} \underline{\psi}U(x) \\ \underline{\psi}L(x+\Delta x) \end{bmatrix}$$

$$+ \begin{bmatrix} \underline{SU}(\Delta x) \\ \underline{SL}(\Delta x) \end{bmatrix} . \tag{2-9}$$

The $\underline{\underline{G}}$ matrix, given by

$$\underline{\underline{G}}(\Delta x) = \begin{bmatrix} \underline{\underline{G}}_{11}(\Delta x) & \underline{\underline{G}}_{12}(\Delta x) \\ \underline{\underline{G}}_{21}(\Delta x) & \underline{\underline{G}}_{22}(\Delta x) \end{bmatrix} ,$$

is normally referred to as the scattering matrix. It along with the vector $\underline{S}$ (Δx) may be determined by writing out the two matrix equations given by Equation (2-7), solving the second equation for $\underline{\psi}L(x)$ and then substituting this value into the first equation. The resulting equations are

$$\underline{\underline{G}}_{11}(\Delta x) = \underline{\underline{\Lambda}}_{11}^{(1)}(\Delta x) - \underline{\underline{\Lambda}}_{12}^{(1)}(\Delta x)[\underline{\underline{\Lambda}}_{22}^{(1)}(\Delta x)]^{-1}[\underline{\underline{\Lambda}}_{21}^{(1)}(\Delta x)] \ , \quad (2\text{-}10a)$$

$$\underline{\underline{G}}_{12}(\Delta x) = \underline{\underline{\Lambda}}_{12}^{(1)}(\Delta x)[\underline{\underline{\Lambda}}_{22}^{(1)}(\Delta x)]^{-1} \ , \quad (2\text{-}10b)$$

$$\underline{\underline{G}}_{21}(\Delta x) = - [\underline{\underline{\Lambda}}_{22}^{(1)}(\Delta x)]^{-1} \underline{\underline{\Lambda}}_{21}^{(1)}(\Delta x) \ , \quad (2\text{-}10c)$$

$$\underline{\underline{G}}_{22}(\Delta x) = [\underline{\underline{\Lambda}}_{22}^{(1)}(\Delta x)]^{-1} \quad (2\text{-}10d)$$

and

$$\underline{SU}(\Delta x) = \underline{FU}(\Delta x) - \underline{\underline{\Lambda}}^{(1)}(\Delta x)[\underline{\underline{\Lambda}}_{22}^{(1)}(\Delta x)]^{-1} \underline{FL}(\Delta x) \ , \quad (2\text{-}11a)$$

$$\underline{SL}(\Delta x) = - [\underline{\underline{\Lambda}}_{22}^{(1)}(\Delta x)]^{-1} \underline{FL}(\Delta x) \ . \quad (2\text{-}11b)$$

For two adjacent intervals whose boundaries are denoted by x_1, x_2, and x_3, Equation (2-9) may be written out giving:

$$\underline{\psi U}(x_2) = \underline{\underline{G}}_{11}(\Delta x_1) \underline{\psi U}(x_1) + \underline{\underline{G}}_{12}(\Delta x_1) \underline{\psi L}(x_2) + \underline{SU}(\Delta x_1) \ , \quad (2\text{-}12a)$$

$$\underline{\psi L}(x_1) = \underline{\underline{G}}_{21}(\Delta x_1) \underline{\psi U}(x_1) + \underline{\underline{G}}_{22}(\Delta x_1) \underline{\psi L}(x_2) + \underline{SL}(\Delta x_1) \ , \quad (2\text{-}12b)$$

$$\underline{\psi U}(x_3) = \underline{\underline{G}}_{11}(\Delta x_2) \underline{\psi U}(x_2) + \underline{\underline{G}}_{12}(\Delta x_2) \underline{\psi L}(x_3) + \underline{SU}(\Delta x_2) \ , \quad (2\text{-}13a)$$

$$\underline{\psi L}(x_2) = \underline{\underline{G}}_{21}(\Delta x_2) \underline{\psi U}(x_2) + \underline{\underline{G}}_{22}(\Delta x_2) \underline{\psi L}(x_3) + \underline{SL}(\Delta x_2) \ , \quad (2\text{-}13b)$$

where $\Delta x_1 = x_2 - x_1$; $\Delta x_2 = x_3 - x_2$. Combining Equations (2-12a) and (2-13b) allows $\psi U(x_2)$ to be written

$$\underline{\psi}U(x_2) = [\underline{I} - \underline{\underline{G}}_{12}(\Delta x_1)\ \underline{\underline{G}}_{21}(\Delta x_2)]^{-1}[\underline{\underline{G}}_{11}(\Delta x_1)\ \underline{\psi}U(x_1)$$

$$+ \underline{\underline{G}}_{12}(\Delta x_1)\ \underline{\underline{G}}_{22}(\Delta x_2)\ \underline{\psi}L(x_3)]$$

$$+ [\underline{I} - \underline{\underline{G}}_{12}(\Delta x_1)\ \underline{\underline{G}}_{21}(\Delta x_2)]^{-1}[\underline{S}U(\Delta x_1)$$

$$+ \underline{\underline{G}}_{12}(\Delta x_1)\ \underline{S}L(\Delta x_2)] \ . \qquad (2\text{-}14a)$$

Similarly combining Equations (2-12b) and (2-13a) allows $\psi L(x_2)$ to be written:

$$\underline{\psi}L(x_2) = [\underline{I} - \underline{\underline{G}}_{21}(\Delta x_2)\ \underline{\underline{G}}_{12}(\Delta x_1)]^{-1}[\underline{\underline{G}}_{22}(\Delta x_2)\ \underline{\psi}L(x_3)$$

$$+ \underline{\underline{G}}_{21}(\Delta x_2)\ \underline{\underline{G}}_{11}(\Delta x_1)\ \underline{\psi}U(x_1)]$$

$$+ [\underline{I} - \underline{\underline{G}}_{21}(\Delta x_2)\ \underline{\underline{G}}_{12}(\Delta x_1)]^{-1}[\underline{S}L(\Delta x_2)$$

$$+ \underline{\underline{G}}_{21}(\Delta x_2)\ \underline{S}U(\Delta x_1)] \ . \qquad (2\text{-}14b)$$

Substitution of Equation (2-14b) into Equation (2-12b) and Equation (2-14a) into Equation (2-13a) determines the recursive relationships needed for collapsing two adjoining scattering matrices and source vectors. These relationships are

$$\underline{\underline{G}}_{11}(\Delta x_1+\Delta x_2) = \underline{\underline{G}}_{11}(\Delta x_2)[\underline{I} - \underline{\underline{G}}_{12}(\Delta x_1)\ \underline{\underline{G}}_{21}(\Delta x_2)]^{-1}\ \underline{\underline{G}}_{11}(\Delta x_1) \ , \qquad (2\text{-}15a)$$

$$\underline{\underline{G}}_{12}(\Delta x_1+\Delta x_2) = \underline{\underline{G}}_{21}(\Delta x_2) + \underline{\underline{G}}_{11}(\Delta x_2)$$

$$\times [\underline{\underline{I}} - \underline{\underline{G}}_{12}(\Delta x_1)\ \underline{\underline{G}}_{21}(\Delta x_2)]^{-1}\ \underline{\underline{G}}_{12}(\Delta x_1)\ \underline{\underline{G}}_{22}(\Delta x_2)\ , \quad (2\text{-}15b)$$

$$\underline{\underline{G}}_{21}(\Delta x_1+\Delta x_2) = \underline{\underline{G}}_{21}(\Delta x_1) + \underline{\underline{G}}_{22}(\Delta x_1)$$

$$\times (\underline{\underline{I}} - \underline{\underline{G}}_{21}(\Delta x_2)\ \underline{\underline{G}}_{12}(\Delta x_1)]^{-1}\ \underline{\underline{G}}_{21}(\Delta x_2)\ \underline{\underline{G}}_{11}(\Delta x_1)\ , \quad (2\text{-}15c)$$

$$\underline{\underline{G}}_{22}(\Delta x_1+\Delta x_2) = \underline{\underline{G}}_{22}(\Delta x_1)[\underline{\underline{I}} - \underline{\underline{G}}_{21}(\Delta x_2)\ \underline{\underline{G}}_{12}(\Delta x_1)]^{-1}\ \underline{\underline{G}}_{22}(\Delta x_2) \quad (2\text{-}15d)$$

and

$$\underline{SU}(\Delta x_1+\Delta x_2) = \underline{SU}(\Delta x_2) + \underline{\underline{G}}_{11}(\Delta x_2)$$

$$\times [\underline{\underline{I}} - \underline{\underline{G}}_{12}(\Delta x_1)\ \underline{\underline{G}}_{21}(\Delta x_2)]^{-1}[\underline{SU}(\Delta x_1)$$

$$+ \underline{\underline{G}}_{12}(\Delta x_1)\ \underline{SL}(\Delta x_2)]\ , \quad (2\text{-}16a)$$

$$\underline{SU}(\Delta x_1+\Delta x_2) = \underline{SL}(\Delta x_1) + \underline{\underline{G}}_{22}(\Delta x_1)$$

$$\times [\underline{\underline{I}} - \underline{\underline{G}}_{21}(\Delta x_2)\ \underline{\underline{G}}_{12}(\Delta x_1)]^{-1}[\underline{SL}(\Delta x_2)$$

$$+ \underline{\underline{G}}_{21}(\Delta x_2)\ \underline{SU}(\Delta x_1)]\ . \quad (2\text{-}16b)$$

The procedure employed to obtain the solution of Equation (2-1) using the transfer-scattering algorithm is straightforward. A calculation is begun by evaluating $\underline{\underline{\Lambda}}^{(1)}(\Delta x')$ and $\underline{\underline{\Lambda}}^{(2)}(\Delta x')$ using Equations

(2-6). The width $\Delta x'$ is related to the width of the first or leftmost interval Δx_1 by

$$\Delta x' = \Delta x_1 / 2^N \ . \tag{2-17}$$

The number of halvings, N, is chosen such that $\underline{\underline{A}}^{(1)}(\Delta x')$ and $\underline{\underline{A}}^{(2)}(\Delta x')$ may be accurately evaluated[9]. Next, Equations (2-10) and (2-11) are used to transform to the scattering matrix formulation. The scattering matrix and source vector for the first interval, i.e., $G(\Delta x_1)$ and $S(\Delta x_1)$, are determined by N successive applications of Equations (2-15) and (2-16).

The scattering matrix and source vector for the remaining intervals are likewise evaluated. After evaluating each interval, its scattering matrix and source vector are collapsed, using Equations (2-15) and (2-16), with the collapsed scattering matrices and source vectors for the preceding intervals. Finally, a system scattering matrix and source vector are determined.

Boundary conditions are introduced using Equation (2-9). If the width of the entire reactor is denoted by Δx, then $\underline{\psi}U(\Delta x)$ and $\underline{\psi}L(x+\Delta x)$ represent the inward directed fluxes on the reactor's left and right boundaries, respectively. Thus, the outward directed fluxes may be determined once the system scattering matrix $\underline{\underline{G}}(\Delta x)$ and source vector $\underline{S}(\Delta x)$ have been obtained. To complete the solution, $\underline{\psi}(x)$ is evaluated at the interior interval boundaries using Equations (2-14).

As noted by Dodds[8], calculation time increased significantly as the number of energy groups, angular segments, or spatial intervals

increased. Hence, the need for an outer iteration scheme to optimize computation time and storage with a flexible group structure.

II. OUTER ITERATION TECHNIQUES

The next section presents a brief review of the outer iteration technique incorporated into the transfer-scattering algorithm by Lillie[10]. The iteration scheme provides a flexible group structure by dividing the G energy groups into P supergroups such that each subgroup contains N_p energy groups. If the supergroup coupling matrix $\underline{B}^p$, state vector $\underline{\psi}^p(x)$, and source vector $\underline{Z}^p(x)$ are defined for each supergroup, Equation (2-3) can be written as a coupled set of P matrix equations:

$$\frac{\partial}{\partial x}\underline{\psi}^p(x) + \underline{B}^p\,\underline{\psi}^p(x) = \underline{Z}^p(x) \qquad (2\text{-}18)$$

$$p = 1, \ldots P .$$

The p'th supergroup state vector $\underline{\psi}^p(x)$ is defined by relating the i'th component to the j'th component of $\underline{\psi}(x)$ defined by Equation (2-2a). Letting

$$I_p = \sum_{\ell=1}^{p} N_\ell$$

gives

$$(\psi^p)_i = (\psi)_j \qquad (2\text{-}19)$$

where

$$i = N_p d - I_p + g; \quad j = G(d-1) + g$$

for

$$g = I_p - N_p + 1, \ldots, I_p; \quad d = 1, \ldots D .$$

The p'th supergroup coupling matrix $\underline{B}^p$ is obtained by removing the inscatter and fission terms from Equation (2-4), leaving

$$(B^p)_{ij} = \frac{1}{\mu_d} (\Sigma_{g'\delta gg'\delta dd'} - T_{gd;\ g'd'w_{d'}}) \tag{2-20}$$

where

$$i = N_p d - I_p + g$$

for

$$g = I_p - N_p + 1, \ldots, I_p; \quad d = 1, \ldots, D$$

and

$$j = N_p d' - I_p + g'$$

for

$$g' = I_p - N_p + 1, \ldots, I_p; \quad d' = 1, \ldots, D .$$

Define the source vector $\underline{Z}^p(x)$ as

$$(Z^p)_i = \frac{1}{\mu_d} \chi_g \sum_{g'=1}^{G} \sum_{d'=1}^{D} (\nu\Sigma_f)_{g'} \phi_{g'd'}(x)\, w_{d'}$$

$$+ \frac{1}{\mu_d} \sum_{g'=1}^{G} \sum_{d'=1}^{D} T_{gd;\ g'd'w_{d'}} \phi_{g'd'}(x)(1-\delta) . \tag{2-21}$$

where

$$i = N_p d - I_p + g; \quad \delta = \begin{cases} 1 \text{ if } g' \text{ is in supergroup } p \\ 0 \text{ otherwise} \end{cases}.$$

The term $\phi_{gd}(x)$ is the interval averaged angular flux. The average flux is obtained by assuming an exponential behavior over the interval and performing a neutron balance across the interval. This requires more computational time, but allows a significant reduction in the number of intervals required.

The outer iteration algorithm uses a residual technique to speed convergence. That is, an eigenvalue calculation is performed to evaluate the residuals in a distributed source calculation. After convergence on an eigenvalue, the interval fission source is approximated by

$$F^{(\infty)} \simeq \sum_{t=1}^{n-1} F^{(t)} + \frac{F^{(n)}}{1 - k^{(n)}} \tag{2-22}$$

where $F^{(t)}$ is the t'th iteration interval fission source and $k^{(n)}$ is the converged eigenvalue. Further discussion of the iterative technique can be found in the work by Lillie[10]. This technique is not applicable to the time-dependent problem. Therefore, it will not be presented in more detail in this thesis.

CHAPTER III

TIME-DEPENDENT TASK SOLUTION SCHEME

To eliminate some of the problems encountered in the previously discussed algorithms, the TASK algorith, developed by Dodds[8,9], will be employed. The outer iteration algorithm, incorporated by Lillie[10], will be used to allow the solution of larger problems. A discussion of the algorithm is presented in the previous chapter.

I. DEVELOPMENT OF THE NUMERICAL MODEL

The time-dependent, multigroup discrete ordinate equation for a homogeneous interval in one dimensional slab geometry and the associated delayed neutron precursor equations for G energy groups, D angular segments, and M delayed neutron precursors are[11]:

$$\frac{1}{v_g}\frac{\partial}{\partial t}\phi_{gd}(x,t) + \Sigma_g\phi_{gd}(x,t) + \mu_d\frac{\partial}{\partial x}\phi_{gd}(x,t) = H_{gd}(x,t) \qquad (3\text{-}1)$$

$$g = 1, \ldots, G; \quad d = 1, \ldots, D$$

where

$$H_{gd}(x,t) = S_{gd}(x,t) + \frac{1}{2}\sum_{i=1}^{M}\lambda_i\,\gamma_g^{\,i}C_i(x,t)$$

$$+ (1-\beta)\,\chi_g\sum_{g'=1}^{G}\sum_{d'=1}^{D}(\nu\Sigma_f)_{g'}\,\phi_{g'd'}(x,t)w_{d'}$$

$$+ \sum_{g'=1}^{G}\sum_{d'=1}^{D}T_{gd;\,g'd'}\,\phi_{g'd'}(x,t)w_{d'}\,, \qquad (3\text{-}2)$$

$$T_{gd;g'd'} = \sum_{\ell=0}^{L} \Sigma_s^{\ell}(g;g') \, P_{\ell}(\mu_d) \, P_{\ell}(\mu_{d'}) \, , \qquad (3\text{-}3)$$

and

$$\frac{\partial}{\partial t} C_i(x,t) = 2\beta_i \sum_{g'=1}^{G} \sum_{d'=1}^{D} (\nu\Sigma_f)_{g'} \, \phi_{g'd'}(x,t) \, w_{d'}$$

$$- \lambda_i \, C_i(x,t) \qquad i = 1, \ldots, M \, . \qquad (3\text{-}4)$$

The symbol $\phi_{gd}(x,t)$ represents the angular flux in group g and angular segment d as a function of the position x and the time t. The time dependent extraneous distributed source in group g and angular segment d is represented by $S_{gd}(x,t)$; μ_d is the average x-direction cosine of the neutron velocity vector, and w_d is equal to half the width of the d'th angular segment. The total cross section and neutron speed for group g are represented by Σ_g and v_g; χ_g represents the fraction of prompt neutrons born in group g, and $(\nu\Sigma_f)_g$ is equal to the number of neutrons born per fission times the fission cross section for group g. The term γ_g^i represents the fraction of delayed neutrons of type i emitted in group g; λ_i is the decay constant of the i'th precursor, and β_i is the fraction of neutrons produced by the ith precursor. The total fraction of delayed neutrons is represented by β. The term $\Sigma_s^{\ell}(g;g')$ is the ℓ'th Legendre component of the scattering cross section for scattering from group g' into group g. The term $P_{\ell}(\mu_d)$ is the ℓ'th ordinary Legendre polynomial evaluated at μ_d and L is equal to the order of scattering anisotrophy. The symbol $T_{gd;g'd'}$ represents the probability of scattering from energy group g' and angular segment d', into energy group g and angular segment d.

Substitute Equation (3-2) into Equation (3-1). After rearrangement there is,

$$\frac{1}{v_g \mu_d} \frac{\partial}{\partial t} \phi_{gd}(x,t) + \frac{\partial}{\partial x} \phi_{gd}(x,t) + \frac{1}{\mu_d} (\Sigma_g - T_{gd;g'd'w_{d'}}) \phi_{gd}(x,t)$$

$$= \frac{1}{\mu_d} S_{gd}(x,t) + \frac{1}{2\mu_d} \sum_{i=1}^{M} \lambda_i \gamma_g^i C_i(x,t)$$

$$+ \frac{(1-\beta)}{\mu_d} \chi_g \sum_{g'=1}^{G} \sum_{d'=1}^{D} (\nu\Sigma_f)_{g'} \phi_{g'd'}(x,t) w_{d'}$$

$$+ \frac{1}{\mu_d} \sum_{g'=1}^{g-1} \sum_{d'=1}^{D} T_{gd;g'd'w_{d'}} \phi_{g'd'}(x,t) \quad . \tag{3-5}$$

If the possibility of upscatter is not considered, the summation of the unscatter source need only include the energy groups corresponding to energy groups with energies higher than the energy of group g.

The outer iteration form of the transfer-scattering algorithm is used to make the most efficient use of computing time and storage. Once the time derivative has been removed from Equation (3-5), the time-dependent transport equation can be cast in the form necessary to employ the transfer-scattering algorithm.

The flux is assumed to vary according to Equation (3-6) over each time step, i.e.,

$$\phi_{gd}(x,t) = e^{\omega_g(x)t} \psi_{gd}(x,t) \quad . \tag{3-6}$$

The true behavior of the flux is approximated by an exponential function and a linear function, $\psi_{gd}(x,t)$. This is commonly referred to as a predictor-corrector form of the flux, that is, the behavior is predicted to vary exponentially and corrected by a linear modifying function.

Substitution of Equation (3-6), into Equation (3-5) and taking the derivative with respect to time yields:

$$\frac{1}{v_g \mu_d} \frac{\partial}{\partial t} \psi_{gd}(x,t) + \frac{\partial}{\partial x} \psi_{gd}(x,t)$$

$$+ \frac{e^{-\omega_g(x)t}}{\mu_d} \left[\Sigma_g - T_{gd;g'd'w_{d'}} + \frac{\omega_g(x)}{v_g} \right] e^{\omega_g(x)t} \psi_{gd}(x,t)$$

$$= \frac{e^{-\omega_g(x)t}}{\mu_d} S_{gd}(x,t) + \frac{e^{-\omega_g(x)t}}{2\mu_d} \sum_{i=1}^{M} \lambda_i \gamma_g^i C_i(x,t)$$

$$+ \frac{e^{-\omega_g(x)t}}{\mu_d} (1-\beta) \chi_g \sum_{g'=1}^{G} \sum_{d'=1}^{D} (\nu\Sigma_f)_{g'} e^{\omega_{g'}(x)t} \psi_{g'd'}(x,t) w_{d'}$$

$$+ \frac{e^{-\omega_g(x)t}}{\mu_d} \sum_{g'=1}^{g-1} \sum_{d'=1}^{D} T_{gd;g'd'w_{d'}} e^{\omega_{g'}(x)t} \psi_{g'd'}(x,t) \quad . \qquad (3\text{-}7)$$

The rearrangement and forward differencing of Equation (3-7) gives:

$$\frac{\psi_{gd}^{j+1}(x) - \psi_{gd}^{j}(x)}{v_g \mu_d \Delta t}$$

$$= - \frac{\partial}{\partial x} \psi_{gd}^{j+1}(x) - \frac{e^{-\omega_g(x)\Delta t}}{\mu_d} \left(\Sigma_g - T_{gd;g'd'w_{d'}} + \frac{\omega_g(x)}{v_g} \right) e^{\omega_g(x)\Delta t} \psi_{gd}^{j+1}(x)$$

$$+ \frac{e^{-\omega_g(x)\Delta t}}{\mu_d} \bar{S}_{gd}(x) + \frac{e^{-\omega_g(x)\Delta t}}{2\mu_d} \sum_{i=1}^{M} \lambda_i \gamma_g{}^i C_i^{j+1}(x)$$

$$+ \frac{e^{-\omega_g(x)\Delta t}}{\mu_d} (1-\beta) \chi_g \sum_{g'=1}^{G} \sum_{d'=1}^{D} (\nu\Sigma_f)_{g'} e^{\omega_{g'}(x)\Delta t} \psi_{g'd'}^{j+1}(x) w_{d'}$$

$$+ \frac{e^{-\omega_g(x)\Delta t}}{\mu_d} \sum_{g'=1}^{g-1} \sum_{d'=1}^{D} T_{gd;g'd'w_{d'}} e^{\omega_{g'}(x)\Delta t} \psi_{g'd'}^{j+1}(x) \qquad (3\text{-}8)$$

where

$$\bar{S}_{gd}(x) = \frac{1}{\Delta t} \int_0^{\Delta t} S_{gd}(x,t)dt \ . \qquad (3\text{-}9)$$

The term Δt is the length of the time step. The superscript refers to the value of the term at the beginning of the time step and j+1 refers to the value at the end of the time step.

Equation (3-8) can be written as:

$$\frac{\partial}{\partial x} \psi_{gd}^{j+1}(x) + \frac{e^{-\omega_g(x)\Delta t}}{\mu_d} \left(\Sigma_g - T_{gd;g'd'w_{d'}} + \frac{1}{v_g} \left[\frac{1}{\Delta t} + \omega_g(x) \right] \right) e^{\omega_g(x)\Delta t} \psi_{gd}^{j+1}(x)$$

$$= \frac{e^{-\omega_g(x)\Delta t}}{\mu_d} \bar{S}_{gd}(x) + \frac{1}{2\mu_d} \sum_{i=1}^{M} \lambda_i \gamma_g{}^i C_i^{j+1}(x) + \frac{1}{v_g \mu_d \Delta t} \psi_{gd}^{j}(x)$$

$$+ \frac{e^{-\omega_g(x)\Delta t}}{\mu_d} (1-\beta)\, \chi_g \sum_{g'=1}^{G} \sum_{d'=1}^{D} (\nu\Sigma_f)_{g'}\, e^{\omega_{g'}(x)\Delta t}\, \psi^{j+1}_{g'd'}(x) w_{d'}$$

$$+ \frac{e^{-\omega_g(x)\Delta t}}{\mu_d} \sum_{g'=1}^{g-1} \sum_{d'=1}^{D} T_{gd;g'd'} w_{d'}\, e^{\omega_{g'}(x)\Delta t}\, \psi^{j+1}_{g'd'}(x) \quad . \tag{3-10}$$

Equation (3-10) is defined in terms of the corrector function, $\psi_{gd}(x)$. In order to redefine Equation (3-10) in terms of the flux, $\psi_{gd}(x)$, define the reference time, t=0, at the beginning of each time step. Based on this definition, Equation (3-6) can be written as

$$\phi^{j}_{gd}(x) = \psi^{j}_{gd}(x) \tag{3-11}$$

and

$$\phi^{j+1}_{gd}(x) = e^{\omega_g(x)\Delta t}\, \psi^{j+1}_{gd}(x) \quad . \tag{3-12}$$

Before proceeding with this derivation, consider selection of the ω_g's of the exponential predictor function. The ω_g's "frequencies"* should be chosen to minimize the error in the solution. There is no obvious method to choose these frequencies, but a method has been successful in practice makes use of the growth of the solution over the previous time step to estimate the exponential behavior over the present time step[12]. This behavior is

$$\omega_g(x) = \frac{1}{\Delta t} \ln \left[\phi^{j}_{g}(x)/\phi^{j-1}_{g}(x)\right] \tag{3-13}$$

---

*The term frequency is used to devote a real valued quantity rather than a complex quantity.

where,

$$\phi_g(x) = 2 \sum_{d=1}^{D} \phi_{gd}(x) w_d \ . \qquad (3\text{-}14)$$

Now proceeding with the derivation, consider Equation (3-10), one supergroup (see Chapter II), at a time. Substitute Equations (3-11) and (3-12) into (3-10) allowing one frequency per supergroup. This eliminates the exponential cross product terms.

$$\frac{\partial}{\partial x} \phi_{gd}^{j+1}(x) + \frac{1}{\mu_d} \left(\Sigma_g - T_{gd;g'd'} w_{d'} + \frac{1}{v_g} \left[\frac{1}{\Delta t} + \omega_g(x) \right] \right) \phi_{gd}^{j+1}(x)$$

$$= \frac{\overline{S}_{gd}(x)}{\mu_d} + \frac{1}{2\mu_d} \sum_{i=1}^{M} \lambda_i \, {}_g C_i^{j+1}(x) + \frac{e^{\omega_g(x)\Delta t}}{v_g \mu_d \Delta t} \phi_{gd}^{j}(x)$$

$$+ \frac{(1-\beta)}{\mu_d} \chi_g \sum_{g'=1}^{G} \sum_{d'=1}^{D} (\nu\Sigma_f)_{g'} \phi_{g'd'}^{j+1}(x) w_{d'}$$

$$+ \frac{1}{\mu_d} \sum_{g'=1}^{g-1} \sum_{d'=1}^{D} T_{gd;g'd'} w_{d'} \phi_{g'd'}^{j+1}(x) \ . \qquad (3\text{-}15)$$

At this point, it is necessary to consider the solution of the delayed neutron precursor equation. Introducing the group averaged scalar flux, given by Equation (3-14), into Equation (3-4) gives:

$$\frac{\partial}{\partial t} C_i(x,t) + \lambda_i C_i(x,t) = \beta_i \sum_{g'=1}^{G} (\nu\Sigma_f)_g \phi_g(x,t) \ . \qquad (3\text{-}16)$$

The same transformation, Equation (3-6) made on the flux in Equation (3-1) is made in Equation (3-16).

$$\frac{\partial}{\partial t} C_i(x,t) + \lambda_i C_i(x,t) = \beta_i \sum_{g=1}^{G} (\nu\Sigma_f)_g \, e^{\omega_g(x)t} \, \psi_{gd}(x,t) \; . \qquad (3\text{-}17)$$

Integration of Equation (3-17) over the time step and rearrangement gives:

$$C_i^{j+1}(x) = C_i^j(x) \, e^{-\lambda_i \Delta t}$$

$$+ \beta_i \sum_{g=1}^{G} \frac{(\nu\Sigma_f)_g}{[\omega_g(x) + \lambda_i]} \left[e^{\omega_g(x)\Delta t} - e^{-\lambda_i \Delta t}\right] \overline{\psi}_g(x) \qquad (3\text{-}18)$$

where,

$$\overline{\psi}_g(x) = \frac{\psi_g^{j+1}(x) + \psi_g^j(x)}{2} \; . \qquad (3\text{-}19)$$

Substitute Equations (3-11) and (3-12) into (3-18)

$$C_i^{j+1}(x) = C_i^j(x) \, e^{-\lambda_i \Delta t}$$

$$+ \frac{\beta_i}{2} \sum_{g=1}^{G} \frac{(\nu\Sigma_f)_g}{[\omega_g(x) + \lambda_i]} \left(e^{\omega_g(x)\Delta t} - e^{-\lambda_i \Delta t}\right) \phi_g^j(x)$$

$$+ \frac{\beta_i}{2} \sum_{g=1}^{G} \frac{(\nu\Sigma_f)_g}{[\omega_g(x) + \lambda_i]} \left(e^{\omega_g(x)\Delta t} - e^{-\lambda_i \Delta t}\right) e^{-\omega_g(x)\Delta t} \phi_g^{j+1}(x) \; .$$

(3-20)

The initial value of $C^j(x)$ is obtained by solving Equation (3-4) for the steady state value of:

$$C_i^{ss}(x) = \frac{\beta_i}{\lambda_i} (\nu\Sigma_f)_g \phi_g^{ss}(x) \tag{3-21}$$

where the superscript (ss) refers to the steady state value of the term.

Equation (3-15) may be written as:

$$\frac{\partial}{\partial x} \phi_{gd}^{j+1}(x) + \frac{1}{\mu_d} \sum_{g'=1}^{G} \sum_{d'=1}^{D} \left(\left(\Sigma_g + \frac{1}{v_g} \left[\frac{1}{\Delta t} + \omega_g(x) \right] \right) \delta_{gg'} \delta_{dd'} - T_{gd;g'd'} w_{d'} \right) \phi_{g'd'}^{j+1}$$

$$= \frac{\overline{S}_{gd}(x)}{\mu_d} + \frac{1}{2\mu_d} \sum_{i=1}^{M} \lambda_i \gamma_g{}^i C_i^{j+1}(x) + \frac{e^{\omega_g(x)\Delta t}}{v_g \mu_d \Delta t} \phi_{gd}^j(x)$$

$$+ \frac{(1-\beta)}{\mu_d} \chi_g \sum_{g'=1}^{G} \sum_{d'=1}^{D} (\nu\Sigma_f)_{g'} \phi_{g'd'}^{j+1}(x) w_{d'}$$

$$+ \frac{1}{\mu_d} \sum_{g'=1}^{g-1} \sum_{d'=1}^{D} T_{gd;g'd'} w_{d'} \phi_{g'd'}^{j+1}(x) . \tag{3-22}$$

The introduction of the state vectors, $\underline{\psi}(x)$ given by

$$\underline{\psi}(x) = [\phi_{11}, \cdots, \phi_{G1}, \cdots, \phi_{gd}, \cdots, \phi_{GD}]^T \tag{3-23}$$

allow Equation (3-22) to be written as

$$\frac{\partial \underline{\psi}^{j+1}(x)}{\partial x} + \underline{\underline{B}}\, \underline{\psi}^{j+1}(x) = \underline{Z}(x) \tag{3-24}$$

where the ij^{th} element of B can be written

$$(B)_{ij} = \frac{1}{\mu_d}\left[\left(\Sigma_{g'} + \frac{1}{v_g}\left(\frac{1}{\Delta t} + \omega_{g'}(x)\right)\right)\delta_{gg'}\delta_{dd'} - T_{gd;g'd'}w_{d'}\right] \tag{3-25}$$

where $i = G(d-1) + g$ for $g = 1, \ldots, G$; $d = 1, \ldots, D$ and $j = G(d'-1) + g'$ for $g' = 1, \ldots, G$; $d' = 1, \ldots, D$. The i^{th} element of the source vector is given by

$$(Z(x))_i = \frac{S_{gd}(x)}{\mu_d} + \frac{1}{2\mu_d}\sum_{i=1}^{M} \lambda_i\, {}^{i}C_i^{j+1}(x) + \frac{e^{\omega_g(x)\Delta t}}{v_g \mu_d \Delta t}\phi_{gd}^{j}$$

$$+ \frac{(1-\beta)}{\mu_d}\chi_g \sum_{g'=1}^{G}\sum_{d'=1}^{D} (\nu\Sigma_f)_{g'}\, \phi_{g\,d}^{j+1}(x) w_{d'}$$

$$+ \frac{1}{\mu_d}\sum_{g'=1}^{g-1}\sum_{d'=1}^{D} T_{gd;g'd'}w_{d'}\, \phi_{g'd'}^{j+1}(x) \; . \tag{3-26}$$

The transport equation has been cast into a form similar to Equation (2-18). The vector manipulations involved in the further development of the equation are identical to those presented in the previous chapter and will not be expounded upon here. Details are presented in Chapter II.

II. THE POINT KINETICS APPROXIMATION

Chapter I contains a review of some of the difficulties of following the prompt drop part of a rod drop transient. The use of the

point kinetics approximation[13,14] in this section will alleviate some of this difficulty.

Consider the one delayed neutron group point kinetics equations,

$$\frac{dn(t)}{dt} = \frac{(\$-1)}{\Lambda}\beta\, n(t) + \lambda C(t) + S \qquad (3\text{-}27)$$

and

$$\frac{dC(t)}{dt} = \frac{\beta}{\Lambda} n(t) - \lambda C(t) \qquad (3\text{-}28)$$

where \$ is reactivity in dollar units, Λ is the neutron generation time, λ is the delayed neutron decay constant, β is the delayed neutron fraction, and $n(t)$ and $C(t)$ are the neutron and precursor concentrations as functions of time. Consider an ideal rod drop in which reactivity changes from an initial value, $\$_i$, to a final value, $\$_f$, instantaneously at time zero. If the system is at steady state prior to the drop, the solution to Equation (3-27) can be written as:

$$n(t) = (\$_f-\$_i)\left[\frac{1}{\$_f(1-\$_f)} e^{w_0 t} - \frac{1}{1-\$_f} e^{w_1 t} - \frac{\$_i}{\$_f(\$_i-\$_f)}\right] n(0) \qquad (3\text{-}29a)$$

where

$$w_0 \simeq \frac{\$_f}{1-\$_f}\lambda \qquad (3\text{-}29b)$$

$$w_1 \simeq -\frac{(1-\$_f)\beta}{\Lambda} \qquad (3\text{-}29c)$$

and $n(0)$ is the steady state neutron density prior to the rod drop.

For times after the drop large in comparison to w_1, the second term in the square brackets of Equation (3-29a) can be ignored leaving

$$n(t) \simeq \left[\frac{\$_f-\$_i}{\$_f(1-\$_f)} e^{w_o t} + \frac{\$_i}{\$_f}\right] n(0) \quad . \tag{3-30}$$

Consider the ratio $n(t)/n(0)$ as t approaches small values relative to w_0.

$$\lim_{t \to 0} \frac{n(t)}{n(0)} = \frac{1-\$_i}{1-\$_f} \quad . \tag{3-31}$$

Equation (3-31) relates the neutron density immediately after the prompt drop the neutron density prior to the rod drop. The solution of the time-dependent transport equation does not yield reactivity directly, but \$ can be related to some known quantities as shown in the following section.

III. NUMERICAL PROCEDURES

The purpose of this section is to present a brief description of the numerical procedures encoded in TDT. A complete description of TDT will not be presented in this thesis, but some knowledge of the computer code can aid in understanding the model.

Each time-dependent problem is preceded by a static eigenvalue calculation or a static fixed source calculation. This static calculation is used to generate the steady state delayed neutron precursor concentration and the pre-rod drop flux. If the initial transient is to be followed, a standard source iteration scheme is employed. The

frequency for the first time step is assumed to be zero. Small time steps are required to follow the transient just as in algorithms discussed in Chapter II.

A convergence acceleration devices are used in TDT. The first is an exponential extrapolation. The exponential behavior of the flux over the previous time step is known from Equation (3-13). The flux is then extrapolated to the center of the present time step by

$$\phi_{gd}^{j+1/2}(x) = \phi_{gd}^{j}(x)\, e^{\omega_g(x)\Delta t/2} \quad . \tag{3-32}$$

The flux in only extrapolated to the center of the time step to reduce overpredictions or underpredictions of the flux. This phenomenon occurs when the flux deviates from a simple exponential behavior. If this device is used to estimate the flux rather than using the previous time step flux, the number of outer iterations required to converge the flux was decreased significantly for the calculations performed for this thesis.

If the initial transient is not to be followed, the point kinetics approximation may be employed. Consider Equation (3-31). The quantity of reactivity, \$, is not calculated directly in the solution process. However, Equation (3-31) can be related to a known quantity, namely the lambda mode eigenvalue which is a direct result of the solution scheme. The reformulated ratio is:

$$\frac{1-\$_i}{1-\$_f} = \frac{[1-(1-\beta)k_i]k_f}{[1-(1-\beta)k_f]k_i} \tag{3-33}$$

where the terms k_i and k_f are the static eigenvalues before and after the step change in reactor cross sections. This calculation requires the calculation of a second eigenvalue, but when computational time is a prime consideration, this approximation is useful. The approximation is only valid for times past the initial transient. Therefore, the initial time step must be large in comparison to the time constants associated with the prompt neutrons. The remainder of the transient is controlled by the decay of the delayed neutron precursors and the size of the time steps can be expanded accordingly.

The initial value of the frequency is given by

$$\omega_g(x) = \frac{1}{\Delta t} \ln \left(\frac{1-\$_i}{1-\$_f}\right) . \qquad (3\text{-}34)$$

Experience has shown that this approximation gives good results.

To prove the validity of the point kinetics assumption, a number of numerical experiements were performed using both models. The results of some of these experiments are presented in the next chapter.

CHAPTER IV

NUMERICAL RESULTS

In order to establish the validity of the time-dependent model presented in the previous chapter, the model was encoded in the outer iteration transport option of the TASK[15] computer code. Rod drop transient problems were evaluated with and without use of the point kinetics approximation. These results were compared to the results obtained by solving the point kinetics equations. The calculation of a transient in a subcritical reactor was performed. This result is compared to TDA[16]. All calculational results presented in this chapter were obtained from calculations performed on an IBM 360 Model 91 computer.

I. COMPARISON WITH POINT KINETICS

In Chapter I, it was stated that the point kinetics model was not valid in loosely coupled reactor cores where local perturbations do not disturb the flux distribution over the entire core. If an integral quantity such as the reactor's power, is considered for relatively small perturbations, the point model should be a good approximation of the time behavior of the system.

The calculational model employed in the first three numerical experiments was a 13 region, one-dimensional model of FTR-3m[17] as shown in Figure 1. The transport calculations were performed using five energy

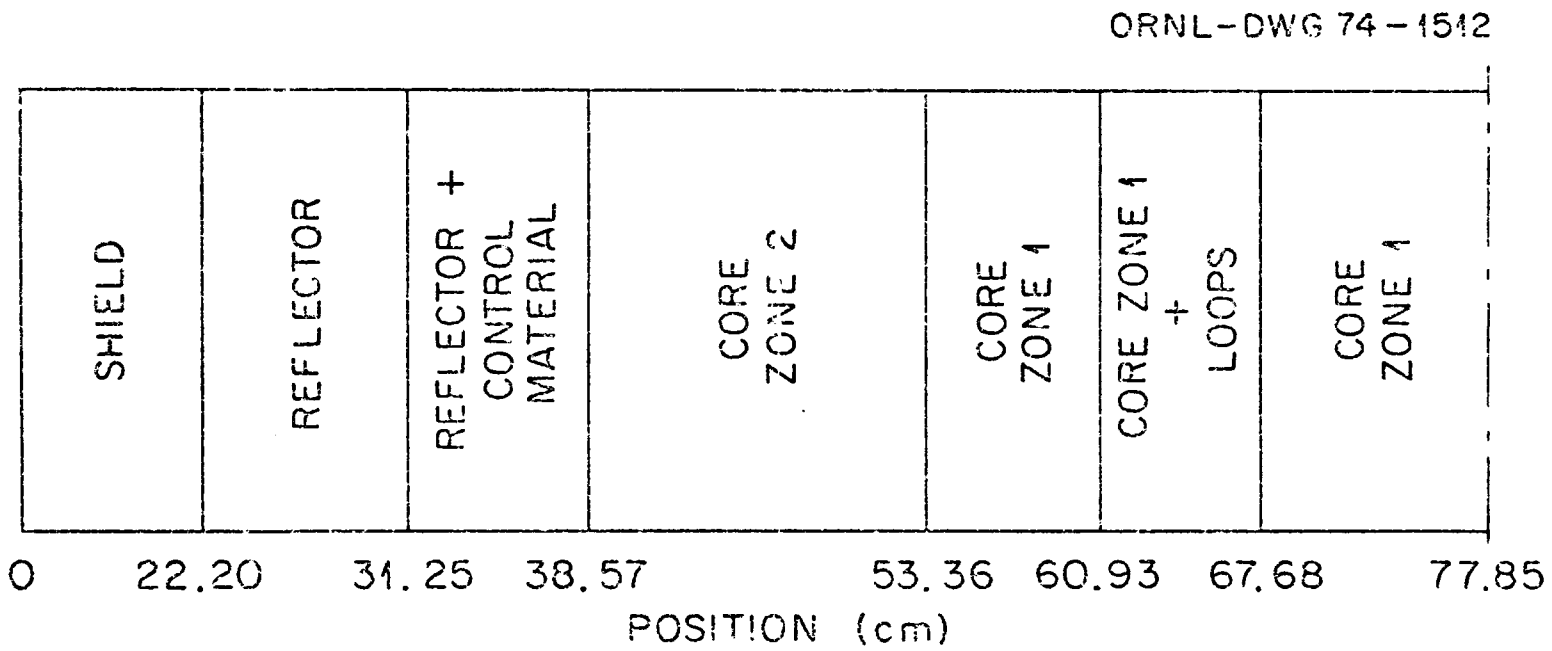


Figure 1. Calculational model--half core mockup of FTR-3m.

groups, an S_4 angular quadrature, and a P_3 expansion of the scattering cross sections. The multigroup constants were generated[18] using the codes ANISN[19] and XSDRN[20]. A conventional $D_g B^2$ buckling correction, where D_g is the diffusion coefficient for group g and B^2 is the transverse geometric buckling, was added to the total cross sections to account for transverse leakage. One group of delayed neutrons was used. The delayed neutron fraction, β, was 0.0032 and the associated decay constant, λ, was 0.08 seconds^{-1}. The point kinetics results were obtained by solving Equation (3-29).

The first numerical experiment was performed using a model where the initial reactivity, $\$_i$, was -3.0932\$ and the final reactivity state, $\$_f$, was -8.4407\$. The neutron generation time, Λ, at this degree of subcriticality was approximately .72 μ seconds[21]. The results of the calculations are presented in Figure 2. The reactivity perturbation was applied symmetrically across the core to minimize the spatial effects of the change. The TDT results are within 1 percent of the point kinetics results.

The second numerical experiment was designed to demonstrate the validity of the solution scheme for a reactor close to critical. The same calculational model employed in the first numerical experiment is employed here. The initial subcriticality of the system is -.1876\$ and the final state is -.9718\$. The neutron generation time at this subcriticality is .75 μ seconds[21]. The results of these calculations are presented in Figure 3. The slight discrepancy between the point kinetics results and the TDT results during the initial transient can be attributed

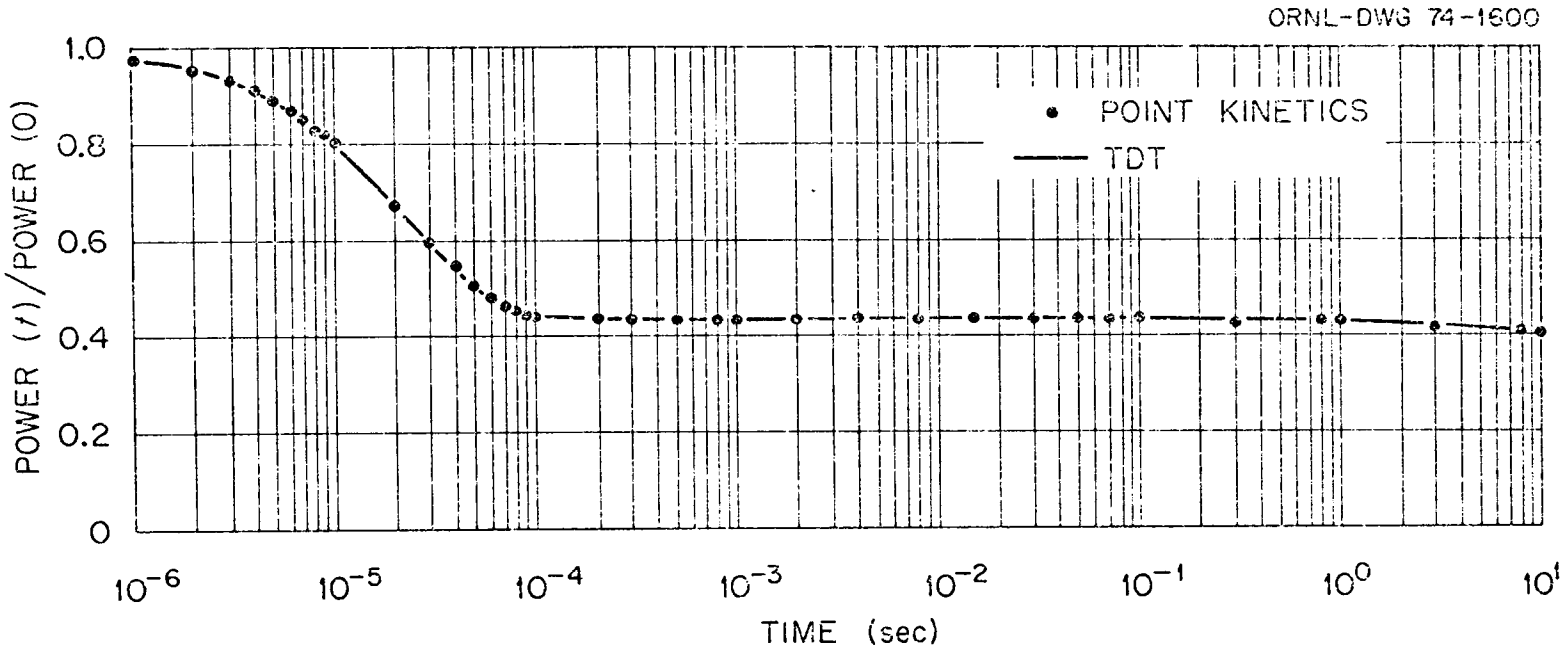


Figure 2. Relative reactor power versus time--TDT and point kinetics calculations--far subcritical.

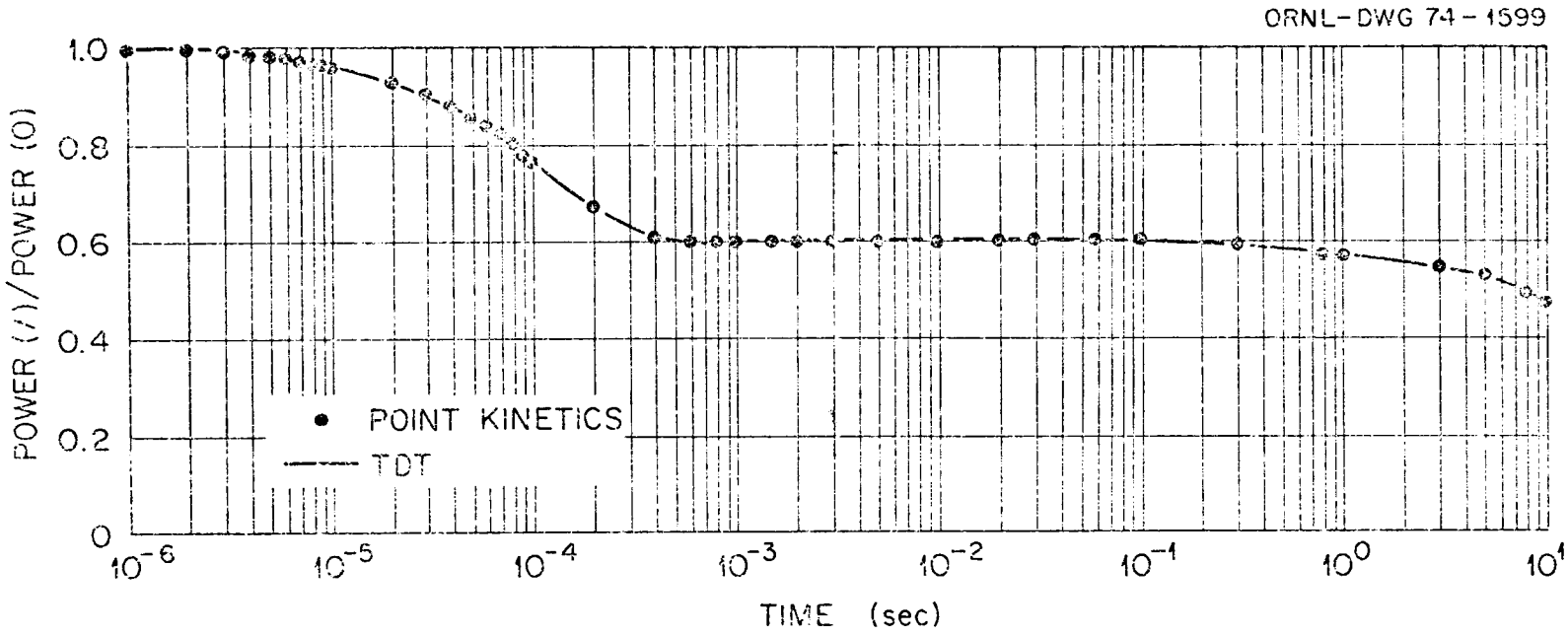


Figure 3. Relative reactor power versus time--TDT and point kinetics calculations--near critical.

to the uncertainty in the neutron generation time. The results are identically the same at times past the initial transient. As before, the TDT results compare within 1 percent of the point kinetics results.

The purpose of the third numerical experiment is to illustrate one of the failures of point kinetics. In the previous experiments, the step change in reactivity used to initiate the transient was applied symmetrically across the reactor to minimize the spatial effects of the perturbation. In this experiment, the perturbation occurs on one side of the reactor. The initial reactivity of the system was -.1876$ and the final reactivity was -5.0490$. The neutron generation time at this subcriticality was approximately .75 μ seconds[21].

Two detectors were located in the reactor shield. Detector #1 was located 68.3 cm. from the center of the core in the shield on the side of the reactor nearest the perturbation. Detector #2 was located in the center of the core. Both detectors were U^{235} fission counters. The result of the TDT calculation and the point kinetics calculation are presented in Figure 4. Previous calculations have shown that the point kinetics model was valid for symmetric perturbations, therefore, the deviation from the point reactor model observed here can be attributed to the spatial and spectral shifts in the flux due to the nonsymmetric perturbation.

The interpretative results of this numerical experiment are presented in Table I. The uncorrected $\$_f$ was obtained by using the uncorrected reaction rates to calculate the reactor's final subcritical state. The detector efficiency was then defined as

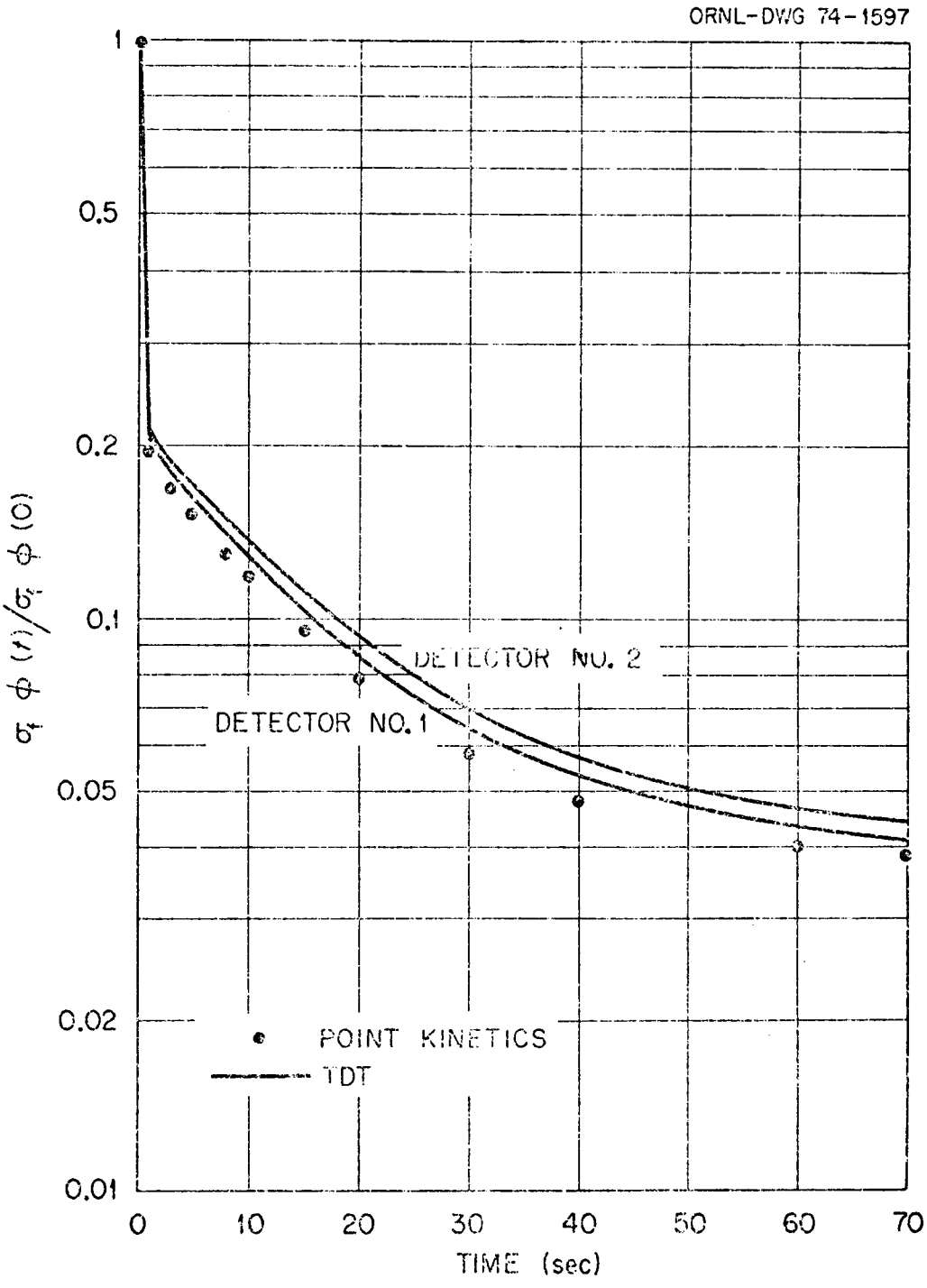


Figure 4. Relative reaction rates versus time--TDT and point kinetics calculations.

TABLE I

INTERPRETATION OF THE SPATIALLY DEPENDENT TEST CASE

Detector	$\$_f$ Uncorrected	$\Delta\$$	$\frac{W_i}{W_f}$	$\$_f$ Corrected	$\%\$$
1	4.793	.256	1.074	4.463	11.6
2	4.398	.651	0.986	4.460	11.7

$$W = \frac{\text{Count Rate}}{\text{Total Fission Rate}} .$$

A first order correction for the spectral shift was made by correcting $\$_f$ by the ratio of the detector efficiency before (W_i) to the detector efficiency after (W_f) the transient. Both detectors indicate the reactor's subcritical state was approximately -4.46\$. This was an 11.6 percent deviation from the true $\$_f$ of -5.049\$. This discrepancy was attributed to a shift in the fundamental distribution of the flux due to the nonsymmetric nature of the rod drop.

For all the experiments presented thus far, it was necessary to use time steps on the order of 3 μ seconds to obtain acceptable results during the initial transient. This requires a relatively large number of time steps to calculate an extremely small span of real time. The use of the optional point kinetics approximation (see Chapter III) made it possible to use an initial time step of 1×10^{-4} seconds. This approximation placed the reactor power on the exponentially decreasing transient following the initial transient. The exponential extrapolation of the flux could then be employed and the time step size appropriately increased until 1 to 2 second time steps were used. The use of still larger time steps was possible at later times during the transients.

II. COMPARISON WITH TDA

To verify the validity of the time model using more than one delayed neutron group, a sample problem was calculated using TDA in which the delayed neutron precursor equations were recently encoded[16]. The

calculational model (see Figure 5) was a hypothetical reactor and was used only as a test problem.

An eigenvalue calculation was performed on a subcritical reactor to obtain the lambda mode flux distribution. The initial delayed neutron precursor distribution was calculated using this flux. The flux was then allowed to decay and the transient was followed.

The model employed in the eigenvalue calculation was a 13 region mockup of a fast reactor. The calculations were performed using six energy groups, an S_2 angular quadrature, and a P_1 expansion of the scattering cross section. All the calculational model parameters including the cross sections are presented in the appendix.

The TDA calculation was performed on an infinite reactor in cylindrical geometry. A cylindrical geometry option is not available in TDT, therefore, it was necessary to add a buckling adjustment to the TDT calculation to achieve the same eigenvalue. The discrepancy in eigenvalue was due to the difference in the amount of neutron leakage from an infinite cylinder and an infinite slab. The geometric buckling was estimated for the slab model and the final calculation performed. The TDA eigenvalue was .903 and the TDT eigenvalue was .897.

The results of the calculations are presented in Figure 6. The slight disagreement between the results of the two calculations can be attributed to the difference in neutron multiplication of the two models. The difference in multiplication is reflected in the eigenvalues. When the results are normalized by the ratio of the system multiplication, the results agree completely.

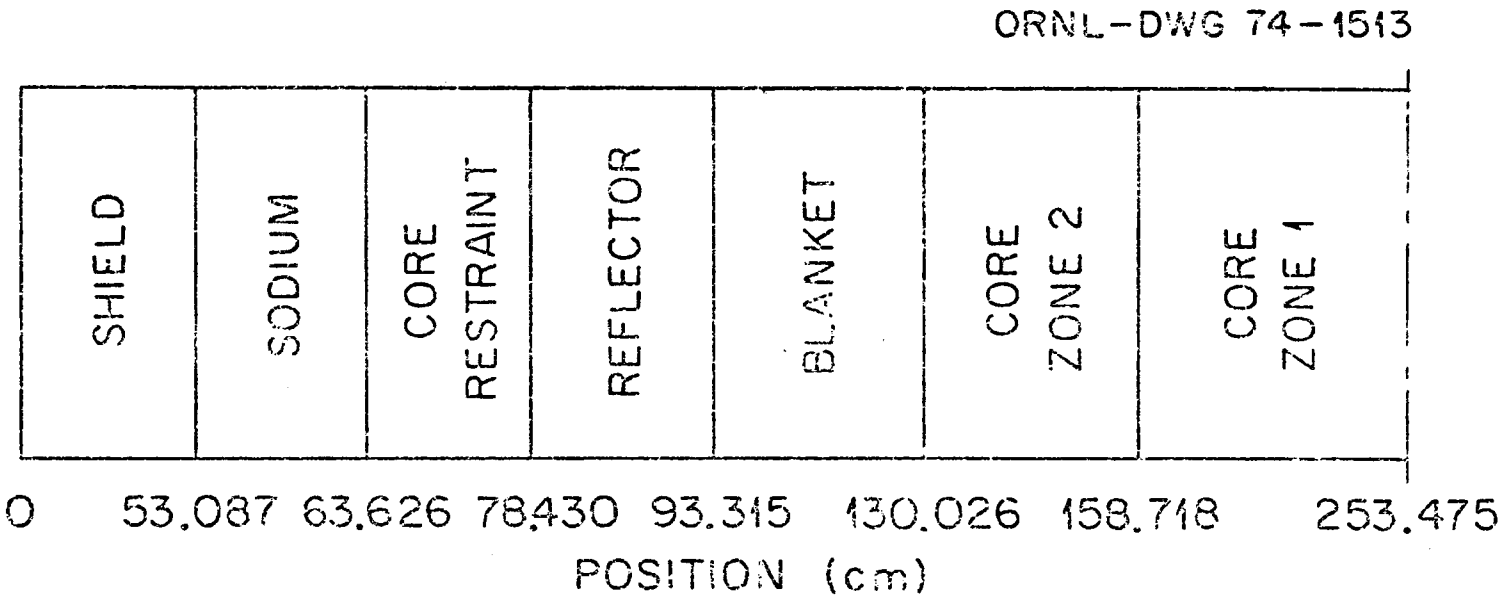


Figure 5. Calculational model--half core model for TDA test problem.

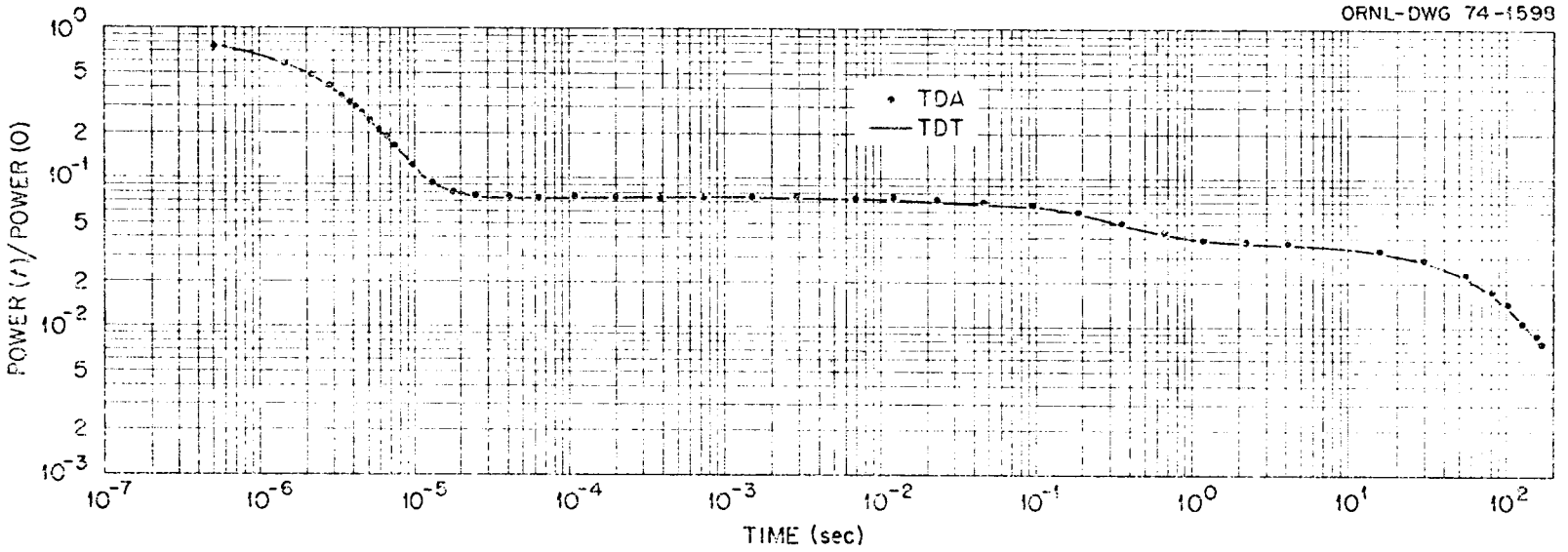


Figure 6. Relative reactor power versus time--TDT and TDA calculations.

There is, however, one significant difference between the two calculations. The TDT calculation required 22.56 minutes of computational time while the TDA calculation required 5.16 minutes. TDA used 65 time steps and TDT used 66 to calculate the same interval of real time, 320 seconds. The increased computational time required by TDT can be attributed to the code's lack of convergence acceleration devices on its outer iteration scheme. Recommendations for further work in this area are presented in the following chapter.

CHAPTER V

SUMMARY

I. CONCLUSIONS

A method has been developed to obtain approximate solutions to the time-dependent Boltzmann neutron transport equation using an existing transfer-scattering algorithm[8]. The method is capable of calculating transients in nuclear reactor cores using the discrete ordinate transport model in one-dimensional slab geometry. A point kinetics approximation was developed for rod drop calculations to eliminate the computationally time consuming initial transient. In addition, a convergence acceleration device is incorporated into the method.

The validity of the coupled algorithm was established by comparing calculated results with results obtained by already existing techniques. In all comparison, the overall agreement was excellent.

II. RECOMMENDATIONS

There are several areas where additional work should be performed. Some recommendations are presented below.

1. The transfer-scattering algorithm developed by Dodds[8] will presently handle either transport or diffusion theory. Thus, an outer iteration scheme and a time-dependent solution capability similar to the iteration scheme developed by Lillie[10]

and the time domain solution method developed in this work, should be coupled to the diffusion theory model.

2. At present, the transfer-scattering algorithm is formulated only to handle vacuum boundary conditions. The incorporation of the capability to handle reflected boundary conditions would reduce the size of symmetric problems by a factor of two.
3. The scattering matrix for each interval and the collapsed scattering matrices (see Chapter II) are not dependent upon the group source vector during a calculation on any given time plane. Thus, the need to evaluate the scattering matrices during each iteration does not exist. Hence, a significant reduction and calculational time may be obtained by storing the scattering matrices out of core, i.e., on a disc pack, rather than reevaluating them each iteration.
4. The source iteration scheme employed in the time dependent solution procedure does not contain an outer iteration convergence acceleration device. Standard power iteration methods such as this tend to converge slowly, especially if the system multiplication factor is close to unity. Thus, an acceleration device is necessary to decrease the number of outer iterations required to converge the flux.

BIBLIOGRAPHY

BIBLIOGRAPHY

1. Kaplan, S., et al., "Space-Time Reactor Dynamics," Proceedings of the Third International Conference on the Peaceful Uses of Atomic Energy, Geneva, 1964, Vol. 4, 41-50, New York: United Nations (1965).

2. Flanagan, G. F., N. M. Greene, W. W. Engle, Jr., E. T. Tomlinson, "Comparison of Transport Approximations for Reactor Physics Calculations in a Fast Reactor," Transactions of the American Nuclear Society, 17: 486-488 (November 1973).

3. Dupree, S. A., H. A. Sandmeir, G. E. Hansen, W. W. Engle, and F. R. Mynatt, "Time-Dependent Neutron and Photon Transport Calculations Using the Method of Discrete Ordinates," LA-4557, Los Alamos Scientific Laboratory (August 1970).

4. Reed, W. H., and K. D. Lathrop, "Truncation Error Analysis of Finite Difference Approximations to the Transport Equation," Nuclear Science and Engineering, 41: 237 (August 1970).

5. Lathrop, K. D., "User's Guide for the TWOTRAN (x,y) Program," LA-4058, Los Alamos Scientific Laboratory (1969).

6. Reed, W. H., "TIMEX: A Time Dependent Explicit Discrete Ordinates Program for the Solution of Multigroup Transport Equations," LA-4800, Los Alamos Scientific Laboratory (July 1972).

7. Reed, W. H., and K. F. Hansen, "Alternating Direction Methods for the Reactor Kinetics Equations," Nuclear Science and Engineering, 41: 431 (1970).

8. Dodds, H. L., Jr., "A New Calculational Method for Space-Energy-Angular Dependent Reactor Kinetics," ORNL-TM-3136, Oak Ridge National Laboratory (January 1971).

9. Dodds, H. L., Jr., J. C. Robinson, and A. R. Buhl, "The Formulation and Application of the Transfer-Scattering Matrix Method to Space-Energy and Angular-Dependent Reactor Kinetics," Nuclear Science and Engineering, 47: 262-274 (March 1972).

10. Lillie, R. A., "Incorporation of Outer Iteration Techniques Into the TASK Algorithm," ORNL-TM-3958, Oak Ridge National Laboratory (November 1972).

11. Swanks, J. H., "Approximate Numerical Solutions to the Time-Dependent Neutron Transport Equations," Unpublished Doctoral Dissertation, The University of Tennessee, Knoxville (1969).

12. Wright, A. L., K. F. Hansen, and D. R. Ferguson, "Application of Alternating-Direction Implicit Methods to the Space-Dependent Kinetics Equations," Nuclear Science and Engineering, 44: 239-251 (1971).

13. Robinson, J. C., The University of Tennessee, Knoxville, Tennessee, personal communication.

14. Yasinsky, J. B., "Notes on Nuclear Reactors Kinetics," WAPD-TM-960, Bettis Atomic Power Laboratory (July 1970).

15. Buhl, A. R., H. D. Dodds, Jr., J. C. Robinson, R. A. Lillie, O. W. Herman and R. J. Hinton, "A User's Manual for TASK, a Generalized One-Dimensional Transport and Diffusion Kinetics Code," ORNL-TM-3811, Oak Ridge National Laboratory (December 1972).

16. Engle, W. W., Oak Ridge National Laboratory, Oak Ridge, Tennessee, personal communication.

17. Buhl, A. R., J. C. Robinson, E. T. Tomlinson, "Intercomparison of Nonperturbing Techniques for Inferring the Reactivity of Fast Reactors," Nuclear Technology 1: 67-74 (January 1974).

18. Buhl, A. R., Oak Ridge National Laboratory, Oak Ridge, Tennessee, personal communication (presently with the Atomic Energy Commission).

19. Engle, W. W., "A User's Manual for ANISN, A One-Dimensional Discrete Ordinates Transport Code with Anistropic Scattering," ORGDP-K-1693, Oak Ridge Gaseous Diffusion Plant (March 1967).

20. Greene, N. M., and C. W. Craven, Jr., "XSDRN: A Discrete Ordinate Spectral Averaging Code," ORNL-TM-2500, Oak Ridge National Laboratory (July 1969).

21. Buhl, A. R., and J. C. Robinson, "Verification of a New Method for Calculating and Measuring Generation Time in a Subcritical Fast Reactor," ORNL-TM-3941, Oak Ridge National Laboratory (September 1972).

APPENDIX

APPENDIX

TDA CALCULATIONAL PARAMETERS

The purpose of this appendix is to present the calculational parameters used in the TDA test problem. The cross sections, prompt neutron fission spectrum, the delayed neutron fission spectrums, the delayed neutron fractions and the decay constant are presented in a region organized format.

The fission neutron spectra and the delayed neutron properties are only presented for the first region since they are the same in all other regions for the problem.

CROSS SECTIONS FOR REGION 1 PLANE HEIGHT = 235.0000 PLANE DEPTH = 235.0000

	INITIAL VALUES			BUCKLING	ADJUSTED VALUES		
GROUP	SIGA	SIGT	NUSIGF	ADJUSTMENT	SIGA	SIGT	1/V CONSTANTS
1	1.35970E-02	2.66750E-01	0.0	4.27069E-04	1.40241E-02	2.67177E-01	5.26315E-10
2	7.07300E-03	3.08660E-01	0.0	3.71313E-04	7.44421E-03	3.09031E-01	5.37630E-10
3	1.78690E-03	2.98660E-01	0.0	3.83253E-04	2.17015E-03	2.99043E-01	5.55550E-10
4	4.26950E-04	2.22520E-01	0.0	5.07476E-04	9.34426E-04	2.23027E-01	5.88230E-10
5	1.57210E-03	5.22070E-01	0.0	2.23019E-04	1.79512E-03	5.22293E-01	3.00000E-09
6	1.05490E-02	9.25350E-01	0.0	1.27089E-04	1.06761E-02	9.25477E-01	2.00000E-08

CROSS SECTIONS FOR REGION 2 PLANE HEIGHT = 235.0000 PLANE DEPTH = 235.0000

	INITIAL VALUES			BUCKLING	ADJUSTED VALUES		
GROUP	SIGA	SIGT	NUSIGF	ADJUSTMENT	SIGA	SIGT	1/V CONSTANTS
1	3.21660E-03	3.45630E-02	0.0	2.49707E-03	5.71387E-03	3.70601E-02	5.26315E-10
2	3.39700E-04	3.84800E-02	0.0	2.31246E-03	3.15216E-03	4.07925E-02	5.37630E-10
3	8.94420E-06	5.19030E-02	0.0	1.84148E-03	1.85043E-03	5.37445E-02	5.55550E-10
4	6.64070E-06	8.63520E-02	0.0	1.20509E-03	1.21172E-03	8.75570E-02	5.88230E-10
5	9.62260E-05	1.27920E-01	0.0	8.49217E-04	9.45443E-04	1.28769E-01	3.00000E-09
6	4.16880E-04	7.10469E-02	0.0	1.42424E-03	1.84112E-03	7.24711E-02	2.00000E-08

CROSS SECTIONS FOR REGION 3 PLANE HEIGHT = 235.0000 PLANE DEPTH = 235.0000

	INITIAL VALUES			BUCKLING	ADJUSTED VALUES		
GROUP	SIGA	SIGT	NUSIGF	ADJUSTMENT	SIGA	SIGT	1/V CONSTANTS
1	3.14510E-02	2.78430E-01	0.0	4.09916E-04	3.18609E-02	2.78840E-01	5.26315E-10
2	2.72290E-02	3.15200E-01	0.0	3.63899E-04	2.75929E-02	3.15564E-01	5.37630E-10
3	1.01700E-02	2.92950E-01	0.0	3.90421E-04	1.05604E-02	2.93340E-01	5.55550E-10
4	6.43930E-04	2.57210E-01	0.0	4.42132E-04	1.08611E-03	2.57652E-01	5.88230E-10
5	2.06390E-03	7.86900E-01	0.0	1.49109E-04	2.21301E-03	7.87049E-01	3.00000E-09
6	9.90700E-03	1.25140E 00	0.0	9.42950E-05	1.00013E-02	1.25149E 00	2.00000E-08

CROSS SECTIONS FOR REGION 4 PLANE HEIGHT = 235.0000 PLANE DEPTH = 235.0000

	INITIAL VALUES			BUCKLING	ADJUSTED VALUES		
GROUP	SIGA	SIGT	NUSIGF	ADJUSTMENT	SIGA	SIGT	1/V CONSTANTS
1	1.23930E-02	2.44950E-01	0.0	4.63249E-04	1.28612E-02	2.45413E-01	5.26315E-10
2	6.54410E-03	2.81000E-01	0.0	4.06323E-04	6.95042E-03	2.81406E-01	5.37630E-10
3	1.95180E-03	2.74530E-01	0.0	4.15459E-04	2.36729E-03	2.74945E-01	5.55550E-10
4	3.83700E-04	2.11890E-01	0.0	5.31523E-04	9.15253E-04	2.12421E-01	5.88230E-10
5	1.42920E-03	4.84320E-01	0.0	2.39972E-04	1.66917E-03	4.84560E-01	3.00000E-09
6	6.34360E-03	7.94100E-01	0.0	1.47777E-04	6.49137E-03	7.94248E-01	2.00000E-08

CROSS SECTIONS FOR REGION 5 PLANE HEIGHT = 235.0000 PLANE DEPTH = 235.0000

GROUP	INITIAL VALUES SIGA	SIGT	NUSIGF	BUCKLING ADJUSTMENT	ADJUSTED VALUES SIGA	SIGT	1/V CONSTANTS
1	6.99970E-04	1.65950E-01	4.99340E-02	6.68360E-04	1.36833E-03	1.66618E-01	5.26315E-10
2	9.46440E-03	1.82650E-01	3.29270E-02	6.08057E-04	1.00725E-02	1.84258E-01	5.37630E-10
3	8.36830E-03	2.10080E-01	2.05380E-02	5.35847E-04	8.90414E-03	2.10616E-01	5.55550E-10
4	2.76960E-03	2.43560E-01	3.15650E-03	4.65764E-04	3.23536E-03	2.44026E-01	5.88230E-10
5	5.53710E-03	3.78740E-01	1.44360E-04	3.04771E-04	5.89187E-03	3.79045E-01	3.00000E-09
6	3.60380E-02	5.64830E-01	8.12150E-04	2.06403E-04	3.62445E-02	5.65036E-01	2.00000E-08

CROSS SECTIONS FOR REGION 6 PLANE HEIGHT = 235.0000 PLANE DEPTH = 235.0000

GROUP	INITIAL VALUES SIGA	SIGT	NUSIGF	BUCKLING ADJUSTMENT	ADJUSTED VALUES SIGA	SIGT	1/V CONSTANTS
1	7.39730E-03	1.38500E-01	3.56480E-02	7.89782E-04	8.18758E-03	1.39290E-01	5.26315E-10
2	8.62860E-03	1.54660E-01	2.50200E-02	7.13482E-04	9.34208E-03	1.55373E-01	5.37630E-10
3	6.94440E-03	1.71250E-01	1.83820E-02	6.49086E-04	7.59348E-03	1.71899E-01	5.55550E-10
4	4.09870E-03	1.86950E-01	9.72690E-03	5.97997E-04	4.69669E-03	1.87548E-01	5.88230E-10
5	5.06400E-03	2.84670E-01	6.37690E-03	4.01305E-04	5.46530E-03	2.85071E-01	3.00000E-09
6	3.51080E-02	4.51050E-01	2.97640E-02	2.57206E-04	3.53652E-02	4.51307E-01	2.00000E-08

CROSS SECTIONS FOR REGION 7 PLANE HEIGHT = 235.0000 PLANE DEPTH = 235.0000

GROUP	INITIAL VALUES SIGA	SIGT	NUSIGF	BUCKLING ADJUSTMENT	ADJUSTED VALUES SIGA	SIGT	1/V CONSTANTS
1	6.50890E-03	1.40800E-01	2.95660E-02	7.77943E-04	7.28684E-03	1.41578E-01	5.26315E-10
2	7.73660E-03	1.57530E-01	2.04650E-02	7.01445E-04	8.43804E-03	1.58231E-01	5.37630E-10
3	6.10650E-03	1.73580E-01	1.45530E-02	6.40959E-04	6.74746E-03	1.74321E-01	5.55550E-10
4	3.61230E-03	1.93570E-01	6.98290E-03	5.78785E-04	4.19108E-03	1.94149E-01	5.88230E-10
5	6.93240E-03	3.01910E-01	4.75280E-03	3.79239E-04	7.31168E-03	3.02289E-01	3.00000E-09
6	5.20420E-02	4.76990E-01	2.25360E-02	2.43569E-04	5.22856E-02	4.77234E-01	2.00000E-08

CROSS SECTIONS FOR REGION 8 PLANE HEIGHT = 235.0000 PLANE DEPTH = 235.0000

GROUP	INITIAL VALUES SIGA	SIGT	NUSIGF	BUCKLING ADJUSTMENT	ADJUSTED VALUES SIGA	SIGT	1/V CONSTANTS
1	7.39780E-03	1.38500E-01	3.56480E-02	7.89782E-04	8.18758E-03	1.39290E-01	5.26315E-10
2	8.62860E-03	1.54660E-01	2.50200E-02	7.13482E-04	9.34208E-03	1.55373E-01	5.37630E-10
3	6.94440E-03	1.71250E-01	1.83820E-02	6.49086E-04	7.59348E-03	1.71899E-01	5.55550E-10
4	4.09870E-03	1.86950E-01	9.72690E-03	5.97997E-04	4.69669E-03	1.87548E-01	5.88230E-10
5	5.06400E-03	2.84670E-01	6.37690E-03	4.01305E-04	5.46530E-03	2.85071E-01	3.00000E-09
6	3.51080E-02	4.51050E-01	2.97640E-02	2.57206E-04	3.53652E-02	4.51307E-01	2.00000E-08

CROSS SECTIONS FOR REGION 9 PLANE HEIGHT = 235.0000 PLANE DEPTH = 235.0000

	INITIAL VALUES			BUCKLING	ADJUSTED VALUES		
GROUP	SIGA	SIGT	NUSIGF	ADJUSTMENT	SIGA	SIGT	1/V CONSTANTS
1	6.99970E-04	1.65950E-01	4.99340E-02	6.68360E-04	1.36833E-03	1.66618E-01	5.26315E-10
2	9.46440E-03	1.83650E-01	3.29270E-02	6.08057E-04	1.00725E-02	1.84258E-01	5.37630E-10
3	8.36830E-03	2.10080E-01	2.05380E-02	5.35047E-04	8.90414E-03	2.10616E-01	5.55550E-10
4	2.78960E-03	2.40360E-01	3.15650E-03	4.65764E-04	3.23536E-03	2.44026E-01	5.88230E-10
5	5.58710E-03	3.78740E-01	1.44360E-04	3.04771E-04	5.89187E-03	3.79045E-01	3.00000E-09
6	3.60380E-02	5.64830E-01	8.12150E-04	2.06493E-04	3.62445E-02	5.65036E-01	2.00000E-08

CROSS SECTIONS FOR REGION 10 PLANE HEIGHT = 235.0000 PLANE DEPTH = 235.0000

	INITIAL VALUES			BUCKLING	ADJUSTED VALUES		
GROUP	SIGA	SIGT	NUSIGF	ADJUSTMENT	SIGA	SIGT	1/V CONSTANTS
1	1.23080E-02	2.44950E-01	0.0	4.63249E-04	1.28612E-02	2.45413E-01	5.26315E-10
2	6.54410E-03	2.81000E-01	0.0	4.06325E-04	6.95042E-03	2.81406E-01	5.37630E-10
3	1.95180E-03	2.74530E-01	0.0	4.15489E-04	2.36729E-03	2.74945E-01	5.55550E-10
4	3.83730E-04	2.11890E-01	0.0	5.31523E-04	9.15253E-04	2.12421E-01	5.88230E-10
5	1.42920E-03	4.84320E-01	0.0	2.39973E-04	1.66917E-03	4.84560E-01	3.00000E-09
6	6.34360E-03	7.94100E-01	0.0	1.47777E-04	6.49137E-03	7.94248E-01	2.00000E-08

CROSS SECTIONS FOR REGION 11 PLANE HEIGHT = 235.0000 PLANE DEPTH = 235.0000

	INITIAL VALUES			BUCKLING	ADJUSTED VALUES		
GROUP	SIGA	SIGT	NUSIGF	ADJUSTMENT	SIGA	SIGT	1/V CONSTANTS
1	3.14510E-02	2.78430E-01	0.0	4.09916E-04	3.18609E-02	2.78840E-01	5.26315E-10
2	2.72290E-02	3.15200E-01	0.0	3.63899E-04	2.76929E-02	3.15564E-01	5.37630E-10
3	1.01700E-02	2.92950E-01	0.0	3.90421E-04	1.05604E-02	2.93340E-01	5.55550E-10
4	6.43930E-04	2.57210E-01	0.0	4.42182E-04	1.08611E-03	2.57652E-01	5.88230E-10
5	2.06290E-03	7.86900E-01	0.0	1.40109E-04	2.21301E-03	7.87049E-01	3.00000E-09
6	9.40700E-03	1.25140E 00	0.0	9.42950E-05	1.00013E-02	1.25149E 00	2.00000E-08

CROSS SECTIONS FOR REGION 12 PLANE HEIGHT = 235.0000 PLANE DEPTH = 235.0000

	INITIAL VALUES			BUCKLING	ADJUSTED VALUES		
GROUP	SIGA	SIGT	NUSIGF	ADJUSTMENT	SIGA	SIGT	1/V CONSTANTS
1	3.21630E-03	3.45630E-02	0.0	2.49707E-03	5.71387E-03	3.70601E-02	5.26315E-10
2	8.39700E-04	3.84800E-02	0.0	2.31246E-03	3.15216E-03	4.07925E-02	5.37630E-10
3	8.94420E-06	5.19030E-02	0.0	1.84148E-03	1.85043E-03	5.37445E-02	5.55550E-10
4	6.64070E-06	8.63520E-02	0.0	1.20508E-03	1.21172E-03	8.75570E-02	5.88230E-10
5	9.62260E-05	1.27920E-01	0.0	8.49217E-04	9.45443E-04	1.28769E-01	3.00000E-09
6	4.16880E-04	7.10469E-02	0.0	1.42424E-03	1.84112E-03	7.24711E-02	2.00000E-08

CROSS SECTIONS FOR REGION 13 PLANE HEIGHT = 235.0000 PLANE DEPTH = 235.0000

GROUP	INITIAL VALUES SIGA	SIGT	NUSIGF	BUCKLING ADJUSTMENT	ADJUSTED VALUES SIGA	SIGT	1/V CONSTANTS
1	1.35970E-02	2.66750E-01	0.0	4.21069E-04	1.40241E-02	2.67177E-01	5.26315E-10
2	7.07300E-03	3.08660E-01	0.0	3.71313E-04	7.44431E-03	3.09031E-01	5.37630E-10
3	1.78690E-03	2.98660E-01	0.0	3.85253E-04	2.17015E-03	2.99043E-01	5.55550E-10
4	4.26950E-04	2.22520E-01	0.0	5.07476E-04	9.34426E-04	2.23027E-01	5.83230E-10
5	1.57210E-03	5.22070E-01	0.0	2.23019E-04	1.79512E-03	5.22293E-01	3.00000E-09
6	1.05490E-02	9.25350E-01	0.0	1.27089E-04	1.06761E-02	9.25477E-01	2.00000E-08

DOWNSCATTER MATRICES BY REGION

REGION 1

GROUP DOWNSCATTER PROBABILITY FOR ORDER 0

(G)	(G TO G)	(G TO G+1)	(G TO G+2)	- - (G TO 6)		
1	1.417E-01	1.177E-02	2.913E-02	5.885E-02	1.341E-02	7.957E-06
2	1.748E-01	3.901E-02	6.488E-02	2.288E-02	2.981E-05	
3	1.982E-01	3.336E-02	1.530E-02	6.739E-06		
4	2.013E-01	2.074E-02	6.573E-06			
5	5.167E-01	3.779E-03				
6	9.148E-01					

GROUP DOWNSCATTER PROBABILITY FOR ORDER 1

1	3.418E-01	1.212E-03	0.0	0.0	0.0	0.0
2	3.926E-01	3.736E-04	0.0	0.0	0.0	
3	3.050E-01	-1.200E-02	0.0	0.0		
4	1.690E-01	-1.179E-02	0.0			
5	4.658E-02	-3.688E-03				
6	3.296E-02					

REGION 2

GROUP DOWNSCATTER PROBABILITY FOR ORDER 0

(G)	(G TO G)	(G TO G+1)	(G TO G+2)	- - (G TO 6)		
1	1.194E-02	5.171E-03	8.084E-03	5.901E-03	2.595E-04	9.881E-10
2	1.650E-02	1.378E-02	6.921E-03	4.444E-04	0.0	
3	3.208E-02	1.754E-02	2.273E-03	0.0		
4	6.764E-02	1.870E-02	0.0			
5	1.262E-01	1.570E-03				
6	7.063E-02					

GROUP DOWNSCATTER PROBABILITY FOR ORDER 1

1	2.612E-02	-1.302E-04	0.0	0.0	0.0	0.0
2	3.109E-02	-2.107E-04	0.0	0.0	0.0	
3	5.219E-02	1.684E-03	0.0	0.0		
4	5.233E-02	-1.583E-02	0.0			
5	1.373E-02	-1.524E-03				
6	6.177E-03					

REGION 3

GROUP DOWNSCATTER PROBABILITY FOR ORDER 0

(G)	(G TO G)	(G TO G+1)	(G TO G+2)	- - (G TO 6)		
1	1.507E-01	1.010E-02	2.564E-02	4.978E-02	1.117E-02	1.676E-05
2	1.812E-01	3.231E-02	5.977E-02	1.468E-02	6.469E-06	
3	1.867E-01	8.195E-02	1.414E-02	1.732E-06		
4	2.385E-01	1.803E-02	1.795E-06			
5	7.788E-01	6.003E-03				
6	1.241E 00					

GROUP DOWNSCATTER PROBABILITY FOR ORDER 1

1	3.595E-01	2.064E-03	0.0	0.0	0.0	0.0
2	3.996E-01	1.734E-03	0.0	0.0	0.0	
3	2.672E-01	-1.116E-02	0.0	0.0		

```
  4  1.397E-01 -1.287E-02  0.0
  5  6.178E-02 -5.860E-03
  6  4.313E-02

                    REGION   4

GROUP               DOWNSCATTER PROBABILITY FOR ORDER  0

 (G)  (G TO G)  (G TO G+1)  (G TO G+2) - - (G TO  6)
  1  1.294E-01  1.165E-02  2.767E-02  5.289E-02  1.187E-02  6.876E-06
  2  1.578E-01  3.692E-02  5.896E-02  2.073E-02  2.841E-05
  3  1.635E-01  7.352E-02  1.555E-02  7.497E-06
  4  1.949E-01  1.659E-02  8.144E-06
  5  4.796E-01  3.256E-03
  6  7.678E-01

GROUP               DOWNSCATTER PROBABILITY FOR ORDER  1
  1  3.135E-01  1.233E-03  0.0        0.0        0.0        0.0
  2  3.548E-01  3.747E-04  0.0        0.0        0.0
  3  2.842E-01 -8.240E-03  0.0        0.0
  4  1.531E-01 -8.564E-03  0.0
  5  4.288E-02 -3.173E-03
  6  2.883E-02

                    REGION   5

GROUP               DOWNSCATTER PROBABILITY FOR ORDER  0

 (G)  (G TO G)  (G TO G+1)  (G TO G+2) - - (G TO  6)
  1  8.204E-02  1.294E-02  9.946E-03  4.422E-02  1.625E-02  1.325E-06
  2  1.011E-01  2.361E-02  3.466E-02  1.482E-02  5.311E-06
  3  1.395E-01  4.652E-02  1.548E-02  1.519E-06
  4  2.123E-01  2.647E-02  2.153E-06
  5  3.722E-01  9.366E-04
  6  5.288E-01

GROUP               DOWNSCATTER PROBABILITY FOR ORDER  1
  1  1.904E-01 -4.966E-03  0.0        0.0        0.0        0.0
  2  2.701E-01 -6.641E-03  0.0        0.0        0.0
  3  2.320E-01 -7.247E-03  0.0        0.0
  4  1.822E-01 -8.710E-05  0.0
  5  5.174E-02 -9.535E-04
  6  2.097E-02

                    REGION   6

GROUP               DOWNSCATTER PROBABILITY FOR ORDER  0

 (G)  (G TO G)  (G TO G+1)  (G TO G+2) - - (G TO  6)
  1  6.870E-02  1.044E-02  1.204E-02  3.101E-02  9.126E-03  1.831E-06
  2  8.460E-02  2.246E-02  2.844E-02  1.052E-02  7.573E-06
  3  1.144E-01  3.896E-02  1.090E-02  2.146E-06
  4  1.651E-01  1.774E-02  2.810E-06
  5  2.790E-01  5.657E-04
  6  4.159E-01
```

```
GROUP                  DOWNSCATTER PROBABILITY FOR ORDER  1
  1  1.609E-01 -2.533E-03  0.0         0.0         0.0         0.0
  2  1.845E-01 -3.594E-03  0.0         0.0         0.0
  3  1.834E-01 -4.553E-03  0.0         0.0
  4  1.358E-01 -2.397E-03  0.0
  5  4.638E-02 -5.575E-04
  6  1.757E-02

                       REGION   7

GROUP                  DOWNSCATTER PROBABILITY FOR ORDER  0

 (G)  (G TO G)  (G TO G+1)  (G TO G+2) - - (G TO  6)
  1  6.957E-02  1.245E-02  1.306E-02  3.051E-03  8.885E-03  1.797E-05
  2  8.550E-02  2.533E-02  2.853E-02  1.042E-02  7.961E-06
  3  1.154E-01  4.163E-02  1.038E-02  2.115E-06
  4  1.698E-01  2.010E-02  2.454E-06
  5  2.944E-01  5.435E-04
  6  4.249E-01

GROUP                  DOWNSCATTER PROBABILITY FOR ORDER  1
  1  1.636E-01 -2.099E-03 -1.713E-07  0.0         0.0         0.0
  2  1.865E-01 -4.905E-03  0.0         0.0         0.0
  3  1.818E-01 -7.510E-03  0.0         0.0
  4  1.373E-01 -4.586E-03  0.0
  5  5.650E-02 -5.272E-04
  6  2.186E-02

                       REGION   8

GROUP                  DOWNSCATTER PROBABILITY FOR ORDER  0

 (G)  (G TO G)  (G TO G+1)  (G TO G+2) - - (G TO  6)
  1  6.870E-02  1.044E-02  1.204E-02  3.101E-03  9.126E-03  1.831E-06
  2  8.430E-02  2.246E-02  2.844E-02  1.032E-02  7.573E-06
  3  1.144E-01  3.896E-02  1.090E-02  2.146E-06
  4  1.651E-01  1.774E-02  2.910E-06
  5  2.790E-01  5.657E-04
  6  4.159E-01

GROUP                  DOWNSCATTER PROBABILITY FOR ORDER  1
  1  1.609E-01 -2.533E-03  0.0         0.0         0.0         0.0
  2  1.845E-01 -3.594E-03  0.0         0.0         0.0
  3  1.834E-01 -4.553E-03  0.0         0.0
  4  1.358E-01 -2.397E-03  0.0
  5  4.638E-02 -5.575E-04
  6  1.757E-02
```

REGION 9

GROUP DOWNSCATTER PROBABILITY FOR ORDER 0

(G)	(G TO G)	(G TO G+1)	(G TO G+2)	- - (G TO 6)		
1	8.204E-02	1.294E-02	9.946E-03	4.422E-02	1.625E-02	1.325E-06
2	1.011E-01	2.361E-02	3.466E-02	1.482E-02	5.311E-06	
3	1.396E-01	4.662E-02	1.548E-02	1.519E-06		
4	2.123E-01	2.847E-02	2.153E-06			
5	3.722E-01	9.366E-04				
6	5.288E-01					

GROUP DOWNSCATTER PROBABILITY FOR ORDER 1

1	1.904E-01	-4.966E-03	0.0	0.0	0.0	0.0
2	2.201E-01	-6.641E-03	0.0	0.0	0.0	
3	2.320E-01	-7.247E-03	0.0	0.0		
4	1.822E-01	-8.710E-05	0.0			
5	5.174E-02	-9.535E-04				
6	2.097E-02					

REGION 10

GROUP DOWNSCATTER PROBABILITY FOR ORDER 0

(G)	(G TO G)	(G TO G+1)	(G TO G+2)	- - (G TO 6)		
1	1.294E-01	1.165E-02	2.767E-02	5.289E-02	1.187E-02	6.876E-06
2	1.578E-01	3.692E-02	5.336E-02	2.073E-02	2.041E-05	
3	1.835E-01	7.352E-02	1.555E-02	7.497E-06		
4	1.949E-01	1.659E-02	8.144E-06			
5	4.796E-01	3.256E-03				
6	7.873E-01					

GROUP DOWNSCATTER PROBABILITY FOR ORDER 1

1	3.135E-01	1.233E-03	0.0	0.0	0.0	0.0
2	3.548E-01	3.747E-04	0.0	0.0	0.0	
3	2.842E-01	-8.240E-03	0.0	0.0		
4	1.531E-01	-8.564E-03	0.0			
5	4.289E-02	-3.173E-03				
6	2.883E-02					

REGION 11

GROUP DOWNSCATTER PROBABILITY FOR ORDER 0

(G)	(G TO G)	(G TO G+1)	(G TO G+2)	- - (G TO 6)		
1	1.507E-01	1.010E-02	2.564E-02	4.979E-02	1.117E-02	1.676E-06
2	1.812E-01	3.231E-02	5.977E-02	1.468E-02	6.469E-06	
3	1.867E-01	8.195E-02	1.414E-02	1.732E-06		
4	2.385E-01	1.803E-02	1.795E-06			
5	7.788E-01	6.003E-03				
6	1.241E 00					

GROUP DOWNSCATTER PROBABILITY FOR ORDER 1

1	3.595E-01	2.064E-03	0.0	0.0	0.0	0.0
2	3.996E-01	1.734E-03	0.0	0.0	0.0	
3	2.672E-01	-1.116E-02	0.0	0.0		
4	1.397E-01	-1.287E-02	0.0			
5	6.178E-02	-5.860E-03				
6	4.313E-02					

REGION 12

GROUP DOWNSCATTER PROBABILITY FOR ORDER 0

(G)	(G TO G)	(G TO G+1)	(G TO G+2)	- - (G TO 6)		
1	1.194E-02	5.171E-03	8.084E-03	5.901E-03	2.595E-04	9.881E-10
2	1.650E-02	1.378E-02	6.921E-03	4.444E-04	0.0	
3	3.208E-02	1.754E-02	2.273E-03	0.0		
4	6.764E-02	1.870E-02	0.0			
5	1.262E-01	1.570E-03				
6	7.063E-02					

GROUP DOWNSCATTER PROBABILITY FOR ORDER 1

1	2.612E-02	-1.302E-04	0.0	0.0	0.0	0.0
2	3.108E-02	-2.107E-04	0.0	0.0	0.0	
3	5.219E-02	1.684E-03	0.0	0.0		
4	5.233E-02	-1.583E-02	0.0			
5	1.373E-02	-1.524E-03				
6	6.177E-03					

REGION 13

GROUP DOWNSCATTER PROBABILITY FOR ORDER 0

(G)	(G TO G)	(G TO G+1)	(G TO G+2)	- - (G TO 6)		
1	1.417E-01	1.177E-02	2.913E-02	5.885E-02	1.341E-02	7.957E-06
2	1.748E-01	3.901E-02	6.488E-02	2.288E-02	2.981E-05	
3	1.982E-01	8.336E-02	1.530E-02	6.739E-06		
4	2.013E-01	2.074E-02	6.573E-06			
5	5.167E-01	3.779E-03				
6	9.148E-01					

GROUP DOWNSCATTER PROBABILITY FOR ORDER 1

1	3.418E-01	1.212E-03	0.0	0.0	0.0	0.0
2	3.926E-01	3.736E-04	0.0	0.0	0.0	
3	3.050E-01	-1.200E-02	0.0	0.0		
4	1.690E-01	-1.179E-02	0.0			
5	4.658E-02	-3.683E-03				
6	3.296E-02					

36* ARRAY 26 ENTRIES READ

37* ARRAY 26 ENTRIES READ

OF

TDA TEST PROBLE4

** FISSION NEUTRON SPECTRA - DELAYED NEUTRON PROPERTIES - FOR REGION 1**

	PROMPT NEUTRONS	DELAYED NEUTRON PRECURSORS 1	2	3	4	5	6
DECAY CONSTANT	--	3.00000E 00	1.00000E-02				
PRECURSOR FRACTION	--	5.00000E-03	5.00000E-03				
FISSION SPECTRUM BY ENERGY GROUP NO.							
1	4.98800E-03	0.0	1.00000E-02				
2	3.28420E-02	2.00000E-02	3.00000E-02				
3	2.61254E-01	2.70000E-01	2.60000E-01				
4	5.70075E-01	6.20000E-01	6.00000E-01				
5	1.30841E-01	9.00000E-02	1.00000E-01				
6	0.0	0.0	0.0				

VITA

Edward Thomas Tomlinson was born in Rockville Centre, New York, on November 7, 1950. He moved with his parents to Wantagh, New York, where he received his elementary and secondary education. He graduated from Wantagh High School in June 1968. In September 1968, he entered The University of Tennessee and in June 1972, he received his Bachelor of Science Degree in Nuclear Engineering. In September 1972, he entered the Graduate School of The University of Tennessee. He is a member of Tau Beta Pi amd Phi Kappa Phi.

He was married to the former Rosemary Vincent of Massapequa, New York, on August 26, 1972.